Response to Reviewers comments on "Secondary ozone peaks in the troposphere over the Himalayas"

Anonymous Reviewer #1

GENERAL COMMENTS: This paper by Ojha et al. presents an interesting study about the occurrence of secondary ozone peaks (SOPs) in the troposphere over the Himalaya/Indian region. The work is mainly based on the combined use of a limited set of vertical ozone sounding available at a single measurement site (Nainital in the Himalayan region) and on the outputs from the EMAC model, with the purposes of elucidating the processes leading to the occurrence of SOPs, characterizing their temporal variability and assessing their contribution to tropospheric ozone. The measurement data at Nainital were also used to evaluate the capacity of EMAC in reproducing SOPs. The paper is well within the scopes of ACP and, potentially, it can seriously help in better clarifying this specific (but rather frequent) tropospheric phenomenon and its implication on tropospheric O3 budget over the region. However, I think that the authors should better take advantage of the long-term (2000 – 2014) EMAC data-set to provide a more robust characterization of this class of events both in terms of their origin, dynamical features and impact on long-term O3 variability. Thus, I recommend publication, but after that some major efforts will be implemented towards this direction. I'm rather confident that the authors can implement the requested changes in a reasonable small amount of time.

Response: We thank the reviewer for the careful evaluation of the manuscript and his/her constructive comments and suggestions. The paper has been revised and now includes more analysis of long-term model simulations, as discussed in responses to the individual comments.

SPECIFIC COMMENTS

Comment 1: In the introduction you should better describe the paramount importance of clarifying processes affecting tropospheric ozone variability in the Southern Asia and Himalayas, two global hot spot for climate, atmospheric composition and anthropogenic pressures (see e.g. http://www.unep.org/pdf/ABCSummaryFinal.pdf).

Response: The suggested information is mentioned in the revised version (Page:3, Lines:86-95) as "Additionally, model simulations are required to both trace the source regions and quantify the effect of SOPs on the tropospheric ozone budget. Such investigations are of key importance as the Indo-Gangetic Plain (IGP) and Himalaya region are global hotspot regions in terms of anthropogenic pressures that could impose threats to Asia's water and food security (Ramanathan et al., ABC report, 2008). Satellite-based studies corroborate the high pollution loading over northern India and the nearby IGP including the Tropospheric Column Ozone (TCO) over South Asia (Fishman et al., 2003).The IGP is a regional hotspot of the so called "Atmospheric Brown Clouds (ABC)", consisting of brown haze formed by sub-micron size aerosol particles, emitted from a wide range of anthropogenic and natural sources. It has been shown that ABC reduce the amount of sunlight reaching the Earth's surface by as much as 10 to 15 %, and enhance atmospheric solar heating by as much as 50% (Ramanathan et al., 2007)."

Comment 2: The verification of EMAC model capacity in reproducing SOP is based on a limited number of vertical soundings (only 6). The comparison provided by Figure 2 is encouraging about the ability of EMAC (despite the relatively coarse horizontal resolution 2.8 x 2.8 deg) in reproducing the SOPs. However, you should mention that this very limited amount of data prevent a systematic assessment. Did you try to inspect soundings at other locations in the same region (e.g. New Delhi, see http://woudc.org/data/explore.php) to make the data-set for verification larger? Can you provide some references of earlier works showing comparison of EMAC vertical ozone profiles with measurements (maybe Jöckel et al, 2016 can be profitably cited)?

Response: The reference to Jöckel et al, 2016 is added for comparison of EMAC ozone fields with aircraft-based measurements from the IAGOS-CARIBIC program (Page: 7, Lines:206). It is shown that the simulation used in this work (RC1SD-base-10a) overestimates ozone concentrations, although mostly in the lower troposphere, while in the tropopause regions a reasonable agreement is obtained, compared to satellite and aircraft observations: "The seasonal cycle is reproduced, but the lower values in the troposphere are generally overestimated by up to 40% by the model. In the stratosphere, differences are smaller, as the model underestimates measurements by 5%, reaching 30% only in summer (Jöckel et al, 2016). Comparison with ozonesondes launched in Delhi has been added in the supplement (Fig. S2), which also shows an overestimation in the lower troposphere. Ozone mixing ratios in the middle troposphere show good agreement with the observations (Page: 7, Lines:204-205).

Comment 3: Pag 6, line 169: I would like to see the bias expressed as %. This would better help in understanding the deviation of the model from the measurements.
Response: Suggestion is incorporated.

Comment 4: Pag 6 line 176: "However, these. . .for completeness". I cannot understand this sentence. Do you mean that the selection by Ojha et al. (2014) is not accurate? Please, rephrase!
Response: No we only meant that the events were identified visually in that paper, while with availability of long-term data in this paper we make a criteria to calculate their frequency. The sentence is rephrased.

Comment 5: It is a pity that the "core" Section "3.2 Origin of SOPs" is discussing only the results from the six selected profiles at Nainital! I strongly encourage the authors to use the 15-year EMAC outputs to investigate in a more systematic way and for a long-term perspective this point. Also the back-trajectories investigation can be carried out for the whole 2000-2014 period by using NCEP re-analysis. I would suggest to use the SOP events identified over the period 2000 – 2014 and aggregate them on a seasonal basis to provide indication about the amount of ozone transported from the stratosphere during SOP (by comparing average O3 , O3s and PV vertical profiles).
Response: Section 3.2 is revised to incorporate the reviewer's suggestions by analyzing 15-year EMAC outputs for a long-term perspective.
Average vertical profile of PV during SOPs, derived from a long-term model simulation (2000–2014), shows similar structure, as shown for the individual events. Average PV values during SOPs are found to be significantly higher (e. g. 3.0±1.3 PVU in winter, 1.8±0.5 during summer monsoon) as compared to timesteps without SOP (0.3±0.2 to 1.5±1.3) (Page: 7, Lines: 219-225 and Supplementary Fig. S3, Table S1).

Evolution of O_3s, O_3 and PV along statistical amount of trajectories is presented (New Fig. 6 in manuscript and Fig. S7, S8 in the supplement). Air masses are enriched the ozone of stratospheric origin during transport to Nainital causing SOPs. A significant fraction of trajectories during non SOP timesteps originates over the south west having lower O_3s (< 90 nmol mol^{-1}). The trajectories which do get higher contributions of stratospheric ozone are found to be diluted during the transport making the enhancements above Nainital too small to be an SOP (Page:8, Lines 264-272).

SOP events identified over the period 2000 – 2014 are aggregated on a seasonal basis and average profiles of O3 , O3s and PV vertical profiles are presented (New Fig. 5, Fig. S3 and Table S1). The amount of ozone transported from the stratosphere during SOPs is also indicated. The average amount of ozone transported from the stratosphere to the SOPs is estimated to be the highest during spring (162.5±40 nmol mol^{-1}), followed by winter (149.4 ± 35 nmol mol-1). In contrast the contribution of tropospheric photochemical sources to the SOPs is highest during the summer monsoon (30 nmol mol^{-1}) (Page-8, Lines:236-239).

Comment 6: Figure 5. Basing on the Figure caption, the TF locations 5 days before the events are reported in the maps. However, all the back-trajectories showed very fast transport: 5 days before the arrival to Nainital the air-masses were (at least) off of the north Africa western coast-lines. Thus, which is the relationship with the identified TFs? I suppose the authors would say that the TF DURING the air-mass transport were reported. . . Moreover, how long the back-trajectories are? No information are provided along the manuscript. . . Also seasonal composites over the period 2000 – 2014 about the spatial locations of tropopause folding related to SOP events can be presented (see e.g. Figure 4 by Putero et al., 2016 but for tropopause crossing). What about days without SOPs? I guess that no (or fewer) tropopause foldings were crossed by back-trajectories for these cases. . .To provide a "climatological" long-term perspective, you should also consider the possibility to present a composite for Fig. 7 and Fig. 8 as a function of the seasons for the period 2000 – 2014.
Response: Yes, we meant TFs DURING the air-mass transport, now clarified in the caption. This figure has been now moved to the supplement (Fig. S4) (Reviewer 2, comment 3). Length of trajectories (5 days) is now mentioned in the section 2.4 as well as in the figure caption. Seasonal composites of the spatial locations of folds (Fig. S6) shows higher frequency of occurrence during SOPs. The days without SOPs have minimal effects of O_3s transport due to fewer folds along the transport path, and dilution of any effects before reaching the Himalayas.

Comment 7: Pag 7, line 228: "This variability in LRT. . ..in Fig.5". It is not clear to me. Please, explain better this kind of association. . .
Response: We meant to say that the dramatic changes in tropopause pressure along the trajectory (e.g. from 100 to 200 hPa on 11th Feb) could be associated with the tropopause folds. The sentence is suitably revised.

Comment 8: Pag 7, line 232: please define "medium".
Response: The folds having a vertical extent of 200 to 350 hPa are defined as medium folds. This is mentioned in the revised manuscript. Further details are available by Škerlak et al. (2015).

Comment 9: Pag. 8, line 241: please provide in the text longitude boundaries for these regions.
Response: Suggestion is incorporated.

Comment 10: Pag 8, line 243: despite your statement at pag 8 line 236, basing on that plot, it looks that a STE is actually occurring also for the June event (a tongue of air-mass rich in O3 extended down to 500 hPa southward than 30N)!
Response: We agree. The statement that stratospheric effect is not found on 7th June is removed. As pointed out by the reviewer, text is also revised considering that some effects also reach southward than 30N (Abstract: Page 1, line 9; Results: Page 9, Lines:303-304; Conclusions: Page: 12, Lines 411-412).

Comment 11: Section 3.4 The authors must provide some information about the long-term SOP trend over the region of interest: this information is very valuable also taking into account the current debate about the occurrence and attribution of tropospheric ozone trends (see e.g. http://www.igacproject.org/TOAR). Trends in seasonal/yearly frequencies or physical features (e.g. altitude) of SOP and the related O3 contribution are detected? Also the information that no long-term trends were detected is nevertheless valuable.
Response: We evaluated trends in SOP frequencies on seasonal and yearly basis, however, as expected due to their origin from dynamical processes, frequency of SOPs discern strong

inter-annual variation as shown in the new Figure S9 in the Supplement. We discuss this in the revised manuscript (Page:13, Lines: 425-429) and provide relevant references.

Comment 12: Figure 10: I would add the percentage contributions of SOPs to monthly TCO values. What the error bars represent?
Response: The percentage contributions of SOPs to monthly TCO values is added. Error bars represent the standard deviation derived from the temporal variations over the period of 2000-2014. Now mentioned in the figure caption.

Comment 13: Conclusions In general this Section reports very important general statements about SOP but which are mostly based on the analysis of just 6 case studies (see lines 323- 220). I would recommend to try to increase the robustness of these interesting hints by adopting a long-term perspective basing on EMAC simulation.
Response: Conclusions are revised to add the additional results based on long-term model simulations (as mentioned in response to comment 5 also) (Page:12, Lines: 395, 399-401).

Comment 14: Line 335: "The minimum in the. . .mixing". I would also mention the northward displacement of subtropical jet stream during summer monsoon.
Response: Suggestion is incorporated.

Comment 15: Line 339: are you able to provide any indication about the impact of this increase in terms of radiative forcing over the region?
Response: Radiative forcing is not explicitly investigated in this paper. To provide an indication, a 4-9 DU higher tropospheric column ozone (due to enhancement at the SOP altitude) would correspond to an increase in surface temperature by 0.07 to 0.16 degree, as we take into account the vertical profile of ozone forcing (Lacis et al., 1990). This is discussed in the revised manuscript (Page: 13, Lines: 422-424).

TECHNICALS
Comment 1: Figure 1. I would skip the typical event plot since it is also reported in Figure 2.
Response: Suggestion is incorporated.

Comment 2: Figure 6: x-axis and y-axis. I suppose the black line is the back-trajectory pressure level: it should be reported in the caption.
Response: Suggestion is incorporated.

Comment 3: Figure 7 (Figure 8): please indicate in the caption the latitude (longitude) value for which the cross section is produced.
Response: Suggestion is incorporated.

Comment 4: Figure 9-10: what the error bars represent?
Response: The error bar in Fig. 9 represents the standard deviation of SOP frequency in each month among different years from 2000-2014 (Page: 10, Lines: 336-337). In Fig. 10 , it shows the standard deviation in the temporal variation of tropospheric ozone column among all the time steps during 2000-2014. This is now added in the figure caption.

References:

Fishman, J., Wozniak, A. E., and Creilson, J. K.: Global distribution of tropospheric ozone from satellite measurements using the empirically corrected tropospheric ozone residual

technique: Identification of the regional aspects of air pollution, Atmos. Chem. Phys., 3, 893-907, doi:10.5194/acp-3-893-2003, 2003.

Jöckel, P., Tost, H., Pozzer, A., Kunze, M., Kirner, O., Brenninkmeijer, C. A. M., Brinkop, S., Cai, D. S., Dyroff, C., Eckstein, J., Frank, F., Garny, H., Gottschaldt, K.-D., Graf, P., Grewe, V., Kerkweg, A., Kern, B., Matthes, S., Mertens, M., Meul, S., Neumaier, M., Nützel, M., Oberländer-Hayn, S., Ruhnke, R., Runde, T., Sander, R., Scharffe, D., and Zahn, A.: Earth System Chemistry integrated Modelling (ESCiMo) with the Modular Earth Submodel System (MESSy) version 2.51, Geosci. Model Dev., 9, 1153-1200, doi:10.5194/gmd-9-1153-2016, 2016.

Lacis, A. A., D. J. Wuebbles, and J. A. Logan (1990), Radiative forcing of climate by changes in the vertical distribution of ozone, J. Geophys. Res., 95(D7), 9971–9981, doi:10.1029/JD095iD07p09971.

Ramanathan, V., Ramana, M. V., Roberts, G., Kim, D., Corrigan, C., Chung, C., and Winker, D.: Warming trends in Asia amplified by brown cloud solar absorption, Nature, 448, doi:10.1038/nature06019, http://dx.doi.org/10.1038/nature06019, 2007.

Ramanathan et al.: Atmospheric Brown Clouds: Regional Assessment Report with Focus on Asia, United Nations Environment Programme, Nairobi, Kenya., 2008.

Škerlak, B., M. Sprenger, S. Pfahl, E. Tyrlis, and H. Wernli, Tropopause folds in ERA-Interim: Global climatology and relation to extreme weather events, J. Geophys. Res. Atmos., 120, 4860–4877, doi:10.1002/2014JD022787, 2015.

Response to Reviewers comments on "Secondary ozone peaks in the troposphere over the Himalayas"

Anonymous Referee #2

GENERAL COMMENTS: The authors use soundings from an Indian station (Nainital) sampled over the course of one year to identify 'secondary ozone peaks' (SOP). According to the authors 3-4 profiles are available per month. Six profiles are presented showing an SOP. A comparison with the EMAC model at T42L90 is used to extend the limited data set over a time period of 15 years (2000-2014) to assess the impact of such events on the ozone column over the Himalayan region. During the monsoon season they find virtually no SOPs over the region of interest. According to the authors such SOPs contribute 7-9 DU of ozone to the tropospheric ozone columns during SOP occurrence. They also show, that the SOPs are only a minor effect and do not significantly enhance the ozone column over the whole year. The quantification of ozone transport across the tropopause is important and as such this study could in principle add to this. Overall the paper is well written and the graphics are clear and appropriate. However, the paper needs some major clarifications: I missed clear descriptions of terms and definitions given the central topic SOP: How do the authors define an SOP? They only provide a definition for the model analysis later in the manuscript, but does this also work for the soundings, which have a much higher resolution? How do they distinguish an SOP from a tropopause fold or do they imply folds as SOPs? This is not clearly stated at all also in the introduction. Directly linked to this they don't discuss the transience or irreversibility of the phenomena, which are however crucial for the irreversibility of ozone flux and the persistence of the effect. I also missed a careful analysis of the transport and mixing process, as stated in the abstract. The authors should and could provide this, but currently they show coincident fields, but not a process. Given these points there I recommend the paper for publication after the following points have been addressed.

Response: We thank the reviewer for the careful evaluation of the manuscript and his/her constructive comments and suggestions. The paper has been revised as discussed in responses to the individual comments.

Major points:

Comment 1: In section 2 the authors should provide a clear definition for SOPs, which have been applied to the soundings. Further: What is the vertical resolution of the soundings and which role does the resolution of the sounding play for definition and the final column ozone estimate? The authors also do not discuss the effect of the limited vertical and horizontal resolution of the model. How many layers do they miss compared to high resolution sonde profile and how would this affect the number of peaks and the ozone column?

Response: SOPs are basically a significant enhancement in ozone mixing ratios as compared to the lower troposphere (by at least 50%). Additionally these are not a direct downward transport and ozone levels above SOPs are again lower (here we considered at least 20%). The defining conditions for SOPs are added in the Section 2 (Page: 5, Lines:148-150).

Sounding data was reported originally at 100 m vertical resolution. As mentioned by the reviewer, the identification of SOP (and their effects) could be affected by the model vertical resolution, if this would be coarser than the vertical extent of SOPs (10-12 km: about 2km). As the EMAC simulations were conducted at a vertical resolution of 0.5 km (i.e. four times finer than the typical SOP extend) by using 90 vertical levels, we are able to reproduce all the six events. It must be stressed that also in the observations SOP were observed both in the high-resolution 100 m sounding data (Ojha et al., 2014) and in the 500-m resolution data (equivalent to model vertical resolution at the tropopause) used for the model evaluation (see Fig. 2).

Moreover, the EMAC modeling system (with the exact same horizontal and vertical resolution) was found capable to reproduce the observed (ERA-Interim) spatiotemporal features of tropopause fold occurrences (Akritidis et al., 2016), indicating that the current model resolution is sufficient for resolving similar processes near the tropopause region.

Comment 2: The authors should pay more attention to the reversibility of the SOPs. As long as the SOPs keep their high PV values as indicated in Figures 2-4, the ozone peaks will not permanently contribute to the tropospheric ozone budget, since they do not mix as shown in Fig.4 by the O3s. Figures 7-9 show O3s structures in the troposphere which are collocated to the tropopause (i.e. PV structure). The authors could e.g. diagnose the evolution of O3S on an isentropic surface relative to the evolution of PV to diagnose a persistent effect of the SOPs on tropospheric ozone. Maybe an additional plot of wind gradients or Richardson number would give some further indication for the process.

Response: The calculations of tropospheric ozone budget are revised by implementing the PV criteria suggested by the reviewer as described in the response to reviewer 2's major comment 4.

Moreover, to investigate the mixing of the transported stratospheric air with tropospheric air in the vicinity of SOPs, we present a turbulence-index (TI) (new Fig. 10), as described in Ellrod and Knapp (1992), to detect Clear Air Turbulence (CAT) areas and potential mixing, similar to the approach followed by Traub and Lelieveld (2003).

The enhanced TI values during the SOPs above Nainital indicate higher probability of mixing between stratospheric and tropospheric air, supporting the irreversible nature of the associated STT (Page: 9,10; Lines: 307-314).

Comment 3: I suggest to calculate a statistical amount of trajectories in the model and to evaluate the evolution of O3s, O3 and PV along the trajectories? I can't see, how the current Lagrangian analysis provides a robust view on any exchange on the basis of one trajectory per case and I suggest to remove Fig.5 and 6. At least the authors could show plots of ozone timeseries along the trajectories in Fig.6. Instead of the current Fig.6 the authors could plot the ratio of O3S/O3 to illustrate the stratospheric entry (with PV as contour to differentiate between transience versus irreversibility). This would much more strengthen the paper. Alternatively the authors could use the ERA Interim data, which drive the EMAC to perform trajectory calculations with a statistical amount of data. This would also much better help to identify the process of ozone transport and mixing into the troposphere by diagnosing PV change.

Response: Statistical amount of trajectories are computed and evolution of O_3s, O_3 and PV is presented (New Figures 6, S7, and S8). Air masses are enriched the ozone of stratospheric origin during transport to Nainital causing SOPs. A significant fraction of trajectories during non SOP timesteps originates over the south west having lower O_3s (< 90 nmol mol^{-1}). The trajectories which do get higher contributions of stratospheric ozone are found to be diluted during the transport making the enhancements above Nainital too small to be an SOP (Page:8, Lines 264-272).

Further, as suggested in place of previous Fig. 6, we show the ratio O_3s/O_3 to illustrate the transport from stratosphere and its advection towards Nainital (Fig. 7 in revised version). This is discussed in the manuscript as "The O_3s/O_3 ratio is mostly found to be close to unity (≥0.9) near the altitude (pressure) of air mass trajectory during transport, except on 7th Jun and 25th Oct (0.5–0.8). The intrusions enriching tropospheric air masses with stratospheric O_3 are clearly visible. More specifically, a significant stratospheric contribution to tropospheric ozone is found in the upper/middle troposphere during the 5-day period before the event, with the associated PV values (< 2 PVU) indicating mixing of stratospheric air into the troposphere" (Page: 9; Lines: 277-282).

Comment 4: For the estimate of the effect of the SOPs on the tropospheric ozone column the authors should extend their analysis. As long as they don't account for the PV change, their results are not related to the tropospheric ozone budget. I suggest to compare in addition to Fig. 10 O3 and O3s for PV < 2 only for periods with and without SOPs. This would give the ozone which stays in the troposphere and leads to an enhancement during periods of SOPs, which would strengthen the importance of the results.
Response: Budget calculation is revised by accounting for PV change (Fig. 12 in the revised manuscript). The effect on tropospheric column ozone is found to be slightly lower (3.3-7.5DU; up to 21%) when PV criteria is applied, as compared to when PV criteria is relaxed and timesteps with PV higher than 2 are also included (4-9 DU; up to 26%) (Page: 12, Lines: 383-389).

Minor comments: l.53: If SOPs occur in the lower stratosphere, how are these defined? They can't be the result of the same mechanism as tropospheric SOPs, are they comparable?
Response: Here we focused on the SOPs in the troposphere. We find that stratosphere troposphere exchange is the main source of SOPs in the troposphere. Differential advection of ozone poor and ozone rich air could lead to secondary ozone peaks in the stratosphere (Lemoine, 2004).

l.100: Whats the output frequency of the model?
Response: 10 hours. Mentioned in the revised version (Page:4, Line: 112). Detailed description of the simulation can be found in Joeckel et al. (2016).

l.117: "Tropopause folds are identified..." : How do the results compare to Sprenger et al,2003 or Skerlak, 2014 (over the Himalayas)?
Response: The mean seasonal (DJF, MAM, JJA, SON) climatology of shallow ($50 \leq \Delta p < 200$ hPa), medium ($200 \leq \Delta p < 350$ hPa) and deep ($\Delta p \geq 350$ hPa) tropopause fold frequencies (%) over the period 2000-2014 are presented (Fig. S5), for intercomparison with the studies of Sprenger et al. (2003) and Škerlak et al. (2015).
The EMAC-simulated fold occurrences are generally in agreement with the findings of the aforementioned studies both spatially and temporally, especially for shallow folds which constitute the majority of folds. Moreover, in agreement with Škerlak et al. (2015), the fold maxima over the Himalayas are found during MAM and DJF, while the minimum fold frequencies are found during JJA.

l.146: Why don't you use a larger number of trajectories and perform a robust analysis?
Response: Trajectories at every time step are computed for May 2002 (the month having highest SOP frequency). Evolution of O_3s, O_3 and PV along the trajectories are analyzed for SOP and No SOP time steps (New Fig. 6, S7, S8). Also see response to your comment 3.

Comment: l.155,156: Why is the model interpolated and not simply evaluated at the model levels, which would avoid interpolation errors particularly in the vertical? Is the output interpolated in time?
Response: Interpolation errors are minimal as model's vertical resolution is also ~500 m on which we are taking the observational profiles for comparison. A time weighted mean of the model profiles have been obtained by weighing higher the profile which is closer in time of the observation (also see Ojha et al., 2016). We suggest (and verified) that this procedure would better include the temporal evolution, as compared to directly taking the profile closest in time.

l.167-172: How do the relative ozone enhancements of compare to the observations instead of the absolute values?

Response: The relative ozone enhancements are also reproduced, in general, with in the variabilities (see Table 1).

l.285-287: 285-287: Clarify: What is meant with" PV structures and subtropical jetstreams"? Do you mean tropopause folds below the jet?

Response: We have modified the phrase in the revised manuscript as follows:"PV structures, induced by fluctuations of the zonal flow and tropopause folds development along the subtropical jet-stream".

References

Akritidis, D., Pozzer, A., Zanis, P., Tyrlis, E., Škerlak, B., Sprenger, M., and Lelieveld, J.: On the role of tropopause folds in summertime tropospheric ozone over the eastern Mediterranean and the Middle East, Atmos. Chem. Phys., 16, 14025-14039, doi:10.5194/acp-16-14025-2016, 2016.

Ellrod, G., and D. Knapp, An objective clear-air turbulence forecasting technique: Verification and operational use, Weather Forecast., 7, 150–165, 1992.

Lemoine, R.: Secondary maxima in ozone profiles, Atmos. Chem. Phys., 4, 1085-1096, doi:10.5194/acp-4-1085-2004, 2004.

Ojha, N., M. Naja, T. Sarangi, R. Kumar, P. Bhardwaj, S. Lal, S. Venkataramani, R. Sagar, A. Kumar, H. C. Chandola: On the processes influencing the vertical distribution of ozone over the central Himalayas: Analysis of yearlong ozonesonde observations, *Atmos. Environ.*, 88, 201-211, ISSN 1352-2310, doi:10.1016/j.atmosenv.2014.01.031, 2014.

Ojha, N., Pozzer, A., Rauthe-Schöch, A., Baker, A. K., Yoon, J., Brenninkmeijer, C. A. M., and Lelieveld, J.: Ozone and carbon monoxide over India during the summer monsoon: regional emissions and transport, Atmos. Chem. Phys., 16, 3013-3032, doi:10.5194/acp-16-3013-2016, 2016.

Sprenger, M., M. Croci Maspoli, and H. Wernli, Tropopause folds and cross-tropopause exchange: A global investigation based upon ECMWF analyses for the time period March 2000 to February 2001, J. Geophys. Res., 108, 8518, doi:10.1029/2002JD002587, D12, 2003.

Škerlak, B., M. Sprenger, S. Pfahl, E. Tyrlis, and H. Wernli, Tropopause folds in ERA-Interim: Global climatology and relation to extreme weather events, J. Geophys. Res. Atmos., 120, 4860–4877, doi:10.1002/2014JD022787, 2015.

Traub, M., and J. Lelieveld, Cross-tropopause transport over the eastern Mediterranean, J. Geophys. Res., 108(D23), 4712, doi:10.1029/2003JD003754, 2003.

Manuscript prepared for Atmos. Chem. Phys.
with version 2014/07/29 7.12 Copernicus papers of the LaTeX class copernicus.cls.
Date: 25 March 2017

Secondary ozone peaks in the troposphere over the Himalayas

Narendra Ojha[1], Andrea Pozzer[1], Dimitris Akritidis[1,2], and Jos Lelieveld[1,3]

[1]Atmospheric Chemistry Department, Max Planck Institute for Chemistry, Mainz, Germany
[2]Department of Meteorology and Climatology, School of Geology, Aristotle University of Thessaloniki, Thessaloniki, Greece
[3]Energy, Environment and Water Research Center, The Cyprus Institute, Nicosia, Cyprus

Correspondence to: Narendra Ojha (narendra.ojha@mpic.de)

Abstract. Layers with strongly enhanced ozone concentrations in the middle-upper troposphere, referred to as Secondary Ozone Peaks (SOPs), have been observed in different regions of the world. Here we use the global ECHAM5/MESSy atmospheric chemistry model (EMAC) to (i) investigate the processes causing SOPs, (ii) explore both their frequency of occurrence and seasonality, and (iii) assess their effects on the tropospheric ozone budget over the Himalayas. The vertical profiles of potential vorticity (PV) and a stratospheric ozone tracer (O_3s) in EMAC simulations, in conjunction with the structure of SOPs, suggest that SOPs over the Himalayas are formed by Stratosphere-to-Troposphere Transport (STT) of ozone. The spatial distribution of O_3s further shows that such effects are in general ~~confined to~~ most pronounced in the northern part of India. Model simulated ozone distributions and backward air trajectories show that ozone rich air masses, associated with STT, originate as far as northern Africa and the North Atlantic Ocean, the Middle-East, as well as nearby regions in Afghanistan and Pakistan, and are rapidly (within 2–3 days) transported to the Himalayas. Analysis of a 15-year (2000-2014) EMAC simulation shows that the frequency of SOPs is highest during the pre-monsoon season (e.g. 11% of the time in May), while no intense SOP events are found during the July-October period. The SOPs are estimated to enhance the Tropospheric Column Ozone (TCO) over the central Himalayas by up to ~~26~~21%.

1 Introduction

Tropospheric ozone is a short-lived climate forcer (Shindell et al., 2012) and an air pollutant with adverse effects on human health and crop yields (Monks et al., 2015, and references therein). The effects of tropospheric ozone on crop yields and human health occur near the surface, whereas its radiative forcing is shown to be strongest in the middle-upper troposphere (e.g. Lacis et al., 1990;

Myhre et al., 2013; Monks et al., 2015). The processes controlling tropospheric ozone in the middle and upper troposphere can be different from those near the surface. The photochemistry involving non-methane volatile organic compounds (NMVOCs) and carbon monoxide, in the presence of nitrogen oxides (NOx) primarily controls ozone pollution in the planetary boundary layer. In contrast, dynamics involving Stratosphere-Troposphere Exchange (STE) play a key role in the middle-upper troposphere (e. g. Holton and Lelieveld, 1996; Lelieveld and Dentener, 2000; Neu et al., 2014; Ojha et al., 2014; Monks et al., 2015). Therefore, to quantify the relative contributions of photochemical and dynamical processes to the ozone budget and assess the climatic impacts of anthropogenic ozone, studies of the vertical distribution of ozone are essential.

Ozone observations have been conducted globally and locally using different instruments and platforms as reviewed recently by Tanimoto et al. (2015). Balloon-borne observations employing ozonesondes offer the advantage of measuring ozone across the tropopause. Analyses of ozonesonde observations have provided valuable information on the variability, general features and trends in ozone profiles (e.g. Logan, 1985, 1994). Secondary maxima in ozone profiles, called Secondary Ozone Peaks (SOPs), are a unique phenomenon in which anomalously large ozone concentrations are observed in confined layers in the middle-upper troposphere or lower stratosphere.

The occurrences of SOPs, underlying processes and their global distribution have been discussed in a limited number of studies (Dobson, 1973; Reid and Vaughan, 1991; Varotsos et al., 1994), reviewed by Lemoine (2004). SOPs have been commonly observed in high latitudes, for example, as laminated structures of ozone with the highest frequency of occurrence during the spring season (Dobson, 1973). These laminated structures are primarily considered to be a winter-spring phenomenon, with a peak altitude of occurrence near 14 km (Reid and Vaughan, 1991). Varotsos et al. (1994) suggested that the north and northwest atmospheric circulations in the lower stratosphere play a key role in the formation of SOPs observed over Athens, Greece. Overall, the occurrence of SOPs is typically considered to be a northern hemispheric phenomenon, with no SOPs reported in the tropics and the southern hemisphere (Lemoine, 2004). Trickl et al. (2011) showed the influences of ozone import from the stratosphere and transport along the subtropical jet stream over Europe. According to the aforementioned studies, SOPs are mainly attributed to dynamical processes involving STE, advection and Rossby wave breaking events.

Recent studies (Hwang et al., 2005, 2007; Park et al., 2012) focusing on the Korean region showed that SOP events regularly occur over mid-latitudes. In contrast to earlier studies ~~presenting~~ that demonstrated the occurrence of SOPs mostly in the lower stratosphere, several SOPs were observed in the upper troposphere over Korea. Hwang et al. (2005) attributed these SOPs to the downward transport of ozone from the stratosphere ~~within~~ on a timescale of about one day (24 h), typical of ~~the~~ cross-tropopause exchange. Furthermore, the frequency of occurrence, estimated from 9 years of ozonesonde observations, was found to have strong seasonal variability over Korea with a broad winter-spring maxima and frequencies of occurrence up to 50–80 % (Hwang et al., 2005). Moreover,

Hwang et al. (2005) reported an increase in SOP occurrences over Korea, while the STT effects are anticipated to increase tropospheric ozone in the future (Banerjee et al., 2016).

The studies pertaining to the influences of STT on the vertical profiles of ozone are relatively sparse over the tropical Indian region. Mandal et al. (1998) analyzed observations from ozonesondes and an MST Radar, and attributed the enhanced ozone mixing ratios in the upper troposphere to STT through the indistinct tropopause over southern India. Fadnavis et al. (2010) combined satellite-borne measurements (TES and MLS) with simulations performed by the MOZART model and showed significant influences of STT over India in particular during winter and spring /pre-monsoon seasons. Venkat Ratnam et al. (2016) used satellite observations to estimate the effect of STE associated with tropical cyclones over the north Indian Ocean. Most of the studies based on in situ measurements have however been confined over the southern part of India (e.g. Mandal et al., 1998; Sinha et al., 2016) and the adjacent marine regions (Lal et al., 2013). Ganguly and Tzanis (2011) used ozonesonde observations from three Indian stations operated by the Indian Meteorological Department (IMD) and suggested that overall STT only plays a minor role into the budget of tropospheric ozone over India. However, the influences of STT were found to increase with latitude /northward over India (Ganguly and Tzanis, 2011).

Studies investigating the SOP structures and implications have been few over the tropical Indian region, until very recently (Ojha et al., 2014; Das et al., 2016). The events over southern India were found to be mainly associated with stratospheric intrusions during tropical cyclonic storms (Das et al., 2016). In contrast, the SOP events observed over the central Himalayas in northern India appear similar to what is typically observed over the mid-high latitudes as mentioned earlier. Moreover, SOPs were observed to be more frequent during spring, and were attributed to the combined effects of STE and advection (Ojha et al., 2014). In the previous work using weekly ozonesonde measurements (3–4 profiles per month), covering the period January 2011–December 2011 (Ojha et al., 2014), only 6 SOP events were observed, being insufficient to calculate the frequency and seasonality of SOP occurrences. Additionally, model simulations are required to both trace the source regions and quantify the effect of SOPs on the tropospheric ozone budget. Such ~~investigation is of critical importance over central Himalayas, as satellite-based studies show~~ investigations are of key importance as the Indo-Gangetic Plain (IGP) and Himalaya region are global hotspot regions in terms of anthropogenic pressures that could impose threats to Asia's water and food security (Ramanathan et al., 2008). Satellite-based studies corroborate the high pollution loading over ~~the~~ northern India and the nearby ~~Indo-Gangetic Plain (IGP)~~ IGP including the Tropospheric Column Ozone (TCO) over South Asia (Fishman et al., 2003). The IGP is a regional hotspot of the so called "Atmospheric Brown Clouds (ABC)", consisting of brown haze formed by sub-micron size aerosol particles, emitted from a wide range of anthropogenic and natural sources. It has been shown that ABC reduce the amount of sunlight reaching the Earth's surface by as much as 10 to 15%, and enhance atmospheric solar heating by as much as 50% (Ramanathan et al., 2007).

In the present study, the global atmospheric chemistry climate model EMAC (ECHAM5/MESSy Atmospheric Chemistry) has been used to explore the processes causing the SOPs, investigate the frequency and seasonality of their occurrence and finally assess their impact on the tropospheric ozone budget over the central Himalayas.

2 Methodology

2.1 EMAC

The ECHAM5/MESSy Atmospheric Chemistry (EMAC) is a numerical system for the simulation of regional and global air quality and climate (Jöckel et al., 2010). In this work the model results from simulation RC1SD-base-10a of the ESCiMo project (Jöckel et al., 2016) are used. The general circulation model ECHAM5 version 5.3.02 (Roeckner et al., 2006) and the Modular Earth Submodel System (MESSy) version 2.51 (Jöckel et al., 2016) were used at T42L90MA-resolution, implying a spherical truncation of T42 (corresponding to a quadratic Gaussian grid of approx. 2.8 by 2.8 degrees in latitude and longitude) and 90 vertical hybrid pressure levels up to 0.01 hPa. The dynamics of the general circulation model were weakly nudged by Newtonian relaxation towards ERA-Interim reanalysis data (Dee et al., 2011). Gas-phase and particulate trace species calculated with the EMAC model have been extensively evaluated in previous studies (e.g. Pozzer et al., 2007, 2010, 2012). Simulation RC1SD-base-10a with model output every 10h, was selected between the ESCiMo simulations as suggested in Jöckel et al. (2016) ("For intercomparison with observations, we recommend to use the results of [...] RC1SD-base-10a."). Detailed information on the model set-up and comparison with observations can be found in Jöckel et al. (2016).

A tracer of stratospheric ozone, denoted as $\mathrm{O_3s}$ in EMAC, has been used to quantify the effects of STT. $\mathrm{O_3s}$ follows the transport and destruction processes of ozone in the troposphere but not its chemical formation (Roelofs and Lelieveld, 1997) and it is initialized to $\mathrm{O_3}$ in the stratosphere.

2.2 Tropopause height and tropopause folds

The Lapse Rate Tropopause (LRT) height is calculated from EMAC output using the WMO definition as the altitude at which lapse rate decreases to a value of 2 ^{o}C/km or less, provided that the average lapse rate between this level and all higher levels within the adjacent 2 km do not exceed 2 ^{o}C/km.

Tropopause folds in EMAC simulations were identified with an algorithm developed by Sprenger et al. (2003), and improved by Ŝkerlak et al. (2014), using the three dimensional fields of potential vorticity, potential temperature and specific humidity. The vertical extent of the folds, as determined by the difference between the upper and middle tropopause crossings (see Fig. 1 in Tyrlis et al. (2014)) has been further used to identify shallow, medium and deep folds, as described and used elsewhere (Tyrlis et al., 2014; Ŝkerlak et al., 2015; Akritidis et al., 2016).

2.3 Observational dataset

The occurrence of SOPs was reported using ozonesonde observations from Nainital (79.45° E, 29.37° N, 1958 m asl), a high altitude station located in the central Himalayan region ~~(Ojha et al., 2014)~~(Fig. 1;(Ojha et al., 2014)). These data have been used to evaluate the capability of EMAC to reproduce SOPs over this region. ~~A typical event~~ Some typical events of SOP occurrence ~~at Nainital observed on 10th March 2011 is shown~~ over Nainital can be seen in Fig. ~~??a~~2. The ozone mixing ratios in the middle-troposphere (10–11 km) are clearly observed to be very high (150–250 nmol mol^{-1}) forming an SOP. The location of Nainital station and the geographical topography of the northern Indian region are also shown in Fig. ~~??b~~1.

Ozone profiles at Nainital were measured using Electrochemical Concentration Cell (ECC) ozonesondes. The method utilizes the titration of ozone in potassium iodide solution, which leads to production of Iodine (I_2). The conversion of I_2 to I^- in the cell leads to the flow of two electrons for each ozone molecule entered. The measured cell current, flow rate of air along with sensor parameters, e.g. the background current and pump temperature, are used to derive ozone mixing ratios (Ojha et al., 2014). The precision and accuracy of ECC-ozonesondes are reported to be $\pm$(3–5)% and $\pm$(5–10)% respectively, up to 30 km altitude (Smit et al., 2007).

The yearlong observations analyzed previously (Ojha et al., 2014) showed six occurrences of elevated ozone layers in the 10–12 km altitude range, identified as SOPs. For the analysis of frequency of occurrence and impacts of SOPs, we classify an ozone profile as SOP, if 1) O_3 mixing ratios at 10–12 km, are higher by at least by 50% compared to average ozone in the lower troposphere and 2) O_3 mixing ratios are again lower (at least by 20%) above the SOP (as shown in Fig. 2 and described in more detail in the section 3.3).

Further details of the Nainital station and meteorology (Sarangi et al., 2014; Singh et al., 2016) and balloon-borne measurements (Smit et al., 2007; Ojha et al., 2014; Naja et al., 2016) can be found elsewhere.

2.4 Backward trajectories

We used the Hybrid Single Particle Lagrangian Integrated Trajectory (HYSPLIT) model (http://ready.arl.noaa.gov/HYSPLIT.php) to investigate the source regions and the transport patterns causing SOPs over the central Himalayas. ~~Backward~~ 5-day backward trajectories have been simulated at 10, 11 and 12 km above sea level (asl) (Fig. S4 in the supplement), which are the typical altitudes ~~where SOPs are observed in this study~~for the 6 SOP events shown in Fig. 2. Additional trajectories have been computed for each model timestep in the month of May 2002 (Fig. 6), during which the model predicts the highest frequency of occurrence in the 2000–2014 period. HYSPLIT trajectory simulations are driven by NCEP reanalysis meteorological fields and the model vertical velocity option has been used for the vertical motions. More details of the backward trajectory simulations

using the HYSPLIT model (Draxler and Hess, 1997, 1998; Draxler et al., 2014) and use of various datasets as meteorological inputs over the Indian region can be found elsewhere (e.g. Ojha et al., 2012; Kumar et al., 2015).

3 Results and Discussion

3.1 Model Evaluation

Fig. 2 shows the comparison of EMAC simulated ozone profiles with ozonesonde measurements over Nainital during six SOP events reported previously (Ojha et al., 2014). Model ozone fields have been bilinearly interpolated to the observation site and model output closer to the time of observation is weighted higher (Ojha et al., 2016). As the vertical resolution of EMAC simulations is about 500–600 m in the middle troposphere (10–12 km), where SOPs are typically observed, the observational values are also shown at similar vertical resolution for comparison. The average ozone mixing ratios along with the corresponding standard deviations for the six events are compared between model and observations in Table 1 for lower, middle and upper tropospheric altitudes.

The EMAC model is found capable of reproducing the altitudinal placement of the SOPs over the central Himalayas during all six events. For example, on 20th Apr and 9th May the model shows the peak ozone mixing ratios at 10.5 km asl, in agreement with the ozonesonde profiles. On other events, such as on 11th Feb, 10th Mar and 25th Oct, the altitude of SOP differs slightly (by 0.5-1 km) between model and ozonesonde profiles, except on 7th Jun (by 2 km). The aforementioned discrepancies in the altitude of SOPs occurrence might be related to the model vertical resolution.

In addition to the altitude of SOPs occurrence, EMAC also quantitatively captures the ozone enhancements. The model bias in simulating peak ozone mixing ratios is found to be varying from about ~~-45 nmol mol^{-1}~~ -26% (7th Jun) to +~~34 nmol mol^{-1}~~ 21% (9th May). The biases are found to be within the variability of 1 standard deviation in 10–12 km altitude (28–59 nmol mol^{-1}) as calculated from ozonesonde observations during spring over this site (See Table 1 and Ojha et al. (2014)).

However, the model generally overestimates the ozone mixing ratios in the lower troposphere by about 11–24 nmol mol^{-1} (Table 1) and shows some limitation in capturing less pronounced SOPs, typically observed outside the winter-spring seasons. The bias in the absolute ozone enhancement (-45 nmol mol^{-1}) as well as in the altitudinal placement of the SOP (by 2 km) are higher on 7th Jun. ~~However, these events were~~ Here EMAC simulations are evaluated for all events identified visually (Ojha et al., 2014)~~and here we show all for completeness~~. The SOP events ~~will be~~ are selected based on specific criteria in order to calculate the frequency of occurrence, as discussed in detail in Sect. 3.3.

Possible biases between model and observations could arise from a variety of sources, most importantly, the time-evolution of the SOPs (Supplementary material - Figure ~~1~~S1). Therefore, the limited number of ozone profile measurements could lead to a temporal difference in the state of

SOP evolution being compared between model and observation. We tried to minimize this effect by applying a weighted average algorithm, as mentioned above.

Overall, ~~because~~ the model is ~~able to reproduce the occurrences~~ found to be able of reproducing the occurrence of SOPs, their altitudinal placements and the ozone enhancements over the central Himalayas. Additionally, EMAC simulated average ozone distribution appears to compare well with the ozonesonde climatology over Delhi (77.16°E, 28.49°N) in north India (Fig. S2) and with aircraft-based measurements from the IAGOS-CARIBIC program (Jöckel et al., 2016). Hence, we use the EMAC simulations to investigate the underlying processes (Section 3.2), the frequency of occurrences (Section 3.3) and the effects on tropospheric ozone budget (Section 3.4).

3.2 Origin of SOPs

In this section, we analyze the EMAC simulated meteorological and chemical fields in conjunction with backward air trajectories to investigate the origin of SOPs over the central Himalayas. Fig. 3 shows the vertical profiles of potential vorticity (PV), a tracer of stratospheric intrusions, during the SOP events observed over Nainital. PV vertical profiles during all SOPs show layers of high values coinciding with the altitude of SOPs.

The enhanced PV layers are found to be weaker during June and October ~~as~~ compared to events during late winter and spring. PV values are found to be between 3.1 PVU (20th Apr) to 4.7 PVU (11th Feb) at the SOP altitudes for the events occurring in winter-spring. Even during the less pronounced events of early-summer and autumn, the PV values at SOP altitude are 1.8–2.5 PVU. ~~The PV values at the SOP altitudes~~ Further, the average vertical profile of PV during SOPs, derived from a long-term model simulation (2000–2014), shows similar structure (Supplementary material- Fig. S3), as shown here for the individual events. Average PV values during SOPs are found to be significantly higher (e. g. 3.0$\pm$1.3 PVU in winter, 1.8$\pm$0.5 PVU during summer monsoon) compared to timesteps without SOP (0.3$\pm$0.2 – 1.5$\pm$1.3 PVU) (Supplementary material- Table S1). Such enhanced PV values during the SOPs suggest that the air masses showing very high ozone levels (SOPs) are of stratospheric origin.

To quantify the amount of ozone transported from the stratosphere during the SOPs, we compare the EMAC simulated vertical profiles of O_3 with O_3s during observed 6 SOP events (Fig. 4). ~~The model shows~~ O_3s values are very similar to O_3 indicating that nearly all ~~excess ozone at the SOP altitudes is of~~ the excess ozone that constitutes SOPs is of the stratospheric origin, ~~during the winter and spring, despite of the fact that the SOPsare below the LRT,~~ except on ~~10th Mar.~~ 7th Jun and 25th Oct. The contribution of tropospheric photochemical sources to the SOPs, as represented by the difference O_3-O_3s, is found to be significant on 25th Oct (15 nmol mol^{-1}) and much larger on 7th Jun (50 nmol mol^{-1}).

The comparison of O_3 with O_3s is further analyzed for the extended period 2000–2014 and a seasonal climatology is derived by aggregating all SOP events into four different seasons (Fig. 5).

The average amount of ozone transported from the stratosphere to the SOPs is found to be the highest during spring (162.5±40 nmol mol^{-1}), followed by winter (149.4±35 nmol mol^{-1}). In contrast the contribution of tropospheric photochemical sources to the SOPs is highest during the summer monsoon (30 nmol mol^{-1}). The stronger anthropogenic contribution up to (and beyond) the SOP altitudes during the summer monsoon could be a combined effect of deep convective mixing towards the onset of the summer monsoon and weak horizontal winds (Ojha et al., 2014; Naja et al., 2016) leading to the accumulation of the photochemically processed air masses of tropospheric origin.

Since the LRT over this region is located significantly higher (Fig. 4, also see Naja et al. (2016)) than the altitude of SOPs, and that the ozone in SOPs is found to be of stratospheric origin, we conclude that stratospheric air masses are sandwiched between tropospheric layers at 10–11 km altitude. This result complements previous studies primarily showing the altitudinal placement of SOPs at about 14 km near the Lower Stratosphere (UTLS) (e.g. Reid and Vaughan, 1991; Hwang et al., 2007).

~~The contribution of tropospheric photochemical sources to the SOPs can be represented by the difference -s, which is found to be large (about 50 nmol mol^{-1}), near SOP altitude on 7th Jun. This could be a combined effect of deep convective mixing towards the onset of the summer monsoon and weak horizontal winds (Ojha et al., 2014; Naja et al., 2016) leading to the accumulation of the photochemically processed air masses of tropospheric origin.~~

In order to investigate the underlying dynamics that transport the stratospheric air masses, leading to the SOPs over the Himalayas, we analyzed the backward air trajectories (~~Fig. ??~~Supplementary material-Fig. S4), initialized over Nainital at 10, 11 and 12 km, which are the typical altitudes of the SOPs (Fig. 2). The air mass trajectories indicate rapid transport from the west, for example on 11th Feb, taking only two days for the air masses to be transported across Africa and Middle-East and reach the Himalayas~~(Fig. ??)~~. Further, the locations of the tropopause folds occurred during the period of air trajectories are also shown. The tropopause folds are mostly found in a belt between about 20 and 35^{o}N, in agreement with previous studies (Ŝkerlak et al., 2015). The air masses have been encountering extensive tropopause dynamics along the path of transport, before reaching the Himalayas.

~~EMAC simulated~~ Additionally, air mass trajectories were computed for each model timestep during May 2002 in which the frequency of SOPs was found to be the highest during the 2000–2014 period. Fig. 6 shows the EMAC simulated evolution of O_3~~vertical profiles along with~~ s along these trajectories classified into SOPs and No SOPs above Nainital. The evolution of O_3 and PV along the trajectories are shown in the supplementary material (Fig. S7 and S8). Air masses are enriched / accumulate the ozone of stratospheric origin during transport to Nainital causing SOPs. A significant fraction of trajectories during non SOP timesteps originates over the south west having lower O_3s (< 90 nmol mol^{-1}). The trajectories which do get higher contributions of stratospheric ozone are found to be diluted during transport, making the enhancements above Nainital too small to be an SOP.

The vertical distribution of EMAC simulated O_3s/O_3 ratio along the 5-day backward air trajectories are shown in Fig. 7. The pressure variations of the air masses and tropopause along the trajectory are also shown. ~~In agreement with the analysis of PV and , there is no apparent downward transport of airmass, as typically observed in altitude variations of the backward trajectories during many STT events (e.g. Ma et al., 2014; Sarangi et al., 2014). Strong~~ The O_3s/O_3 ratio is mostly found to be close to unity ($\geq$0.9) near the altitude (pressure) of air mass trajectory during transport, except on 7th Jun and 25th Oct (0.5–0.8). The intrusions enriching tropospheric air masses with stratospheric O_3 are clearly visible. More specifically, a significant stratospheric contribution to tropospheric ozone is found in the upper/middle troposphere during the 5-day period before the event, with the associated PV values (< 2 pvu) indicating mixing of stratospheric air into the troposphere. Additionally, strong variability in the altitude of the LRT along the path of the transport is seen, except for the event of 7th Jun. ~~This variability in LRT~~ The dramatic variability in the LRT along the trajectory (e.g. from 100 to 200 hPa on 11th Feb) appears to be associated with the tropopause ~~folds as shown in Fig. ??~~folding activity (Fig. S4 and S5). Several shallow tropopause folds ~~are seen~~ (vertical extent of 50 to 200 hPa) occur along the transport path, while ~~deeper folds (medium~~medium folds (vertical extent of 200–350 hPa) are only ~~seen~~ found during 11th Feb and 9th May~~(also see Ŝkerlak et al. (2015))~~. Intrusion of a significant amount of O_3 due to tropopause folds over the Eastern Mediterranean and the Middle-East was shown by Akritidis et al. (2016). The combination of very strong winds associated with the subtropical jets (Fig. ~~??~~S4, (Ojha et al., 2014; Naja et al., 2016)) and this intense tropopause dynamics, enriching the troposphere with stratospheric ozone, leads to the formation of SOPs over the Himalayas. ~~Transport of stratospheric air during the analysis period is not found on 7th Jun (Fig. 7), which explains the smaller ozone enhancement in this event, probably related to the presence of some residual influences from previous days (Fig. ?? and 7).~~

The transport of ozone rich air masses from the stratosphere towards the Himalayas can be seen more clearly in the longitude-pressure cross sections at 30^{o}N (Fig. 8), and latitude-pressure cross sections at 80^{o}E (Fig. 9) for all the events and the day before. Fig. 8 reveals three geographical regions viz. Northern Africa and Atlantic Ocean (lon < 40^{o}E), Middle-East (40^{o}E–60^{o}E) and northern South Asia (60^{o}E–100^{o}E), where the intrusions of stratospheric air masses can be identified. Blobs of air masses characterized by high PV values (> 2 PVU) are also seen. Additionally, Fig. 9 shows ~~a strong disparity in the stratospheric influences at 80^{o}E, with effects of STT mostly confined at latitudes higher than 25^{o}N, and minimal over the~~ that stratospheric influences are more pronounced over the northern parts of the Indian subcontinent compared to Southern India. This result based on EMAC simulations is found to be in agreement with the study by Ganguly and Tzanis (2011) based on ozonesonde observations at three Indian stations.

To investigate the possible mixing of the transported stratospheric air with tropospheric air in the vicinity of the SOPs, the Turbulence-Index (TI) is derived from EMAC fields, as described in Ellrod and Knapp (1992). To detect the Clear Air Turbulence (CAT) areas and potential mixing,

the approach similar to Traub and Lelieveld (2003) has been followed. The pressure-longitude cross sections of O_3s (color filled) and TI (contour lines) at 29.5°N near the SOPs pressure height (400-100 hPa) are shown in the Fig. 10 for the timesteps of events and a timestep before and after the event. The enhanced TI values during the SOP events above Nainital indicate higher probability of mixing between stratospheric and tropospheric air, supporting the irreversible nature of the associated STT.

3.3 Frequency of SOPs

The frequency of SOP occurrences was not estimated over Nainital from observations, due to the availability of only 3-4 profiles in each month, however a tendency of higher frequency during spring was noticed (3 events), as compared to other seasons (1 event per season) (Ojha et al., 2014). In this section, we use long-term EMAC simulations, conducted for a period of 15 years (2000–2014), to investigate the frequency of SOP occurrence and seasonality over the central Himalayas. Due to the variability in the SOP altitude as well as the absolute enhancements during the SOPs, general / unique criteria can not be defined. Therefore, we first select the ozone profiles in which Average Ozone Mixing Ratios (AOMR) at 10–12 km, a typical altitude of SOP occurrence, are significantly higher (at least by 50%) compared to average ozone in the lower troposphere. Additionally, to explicitly select only the profiles which are SOPs (and not a direct intrusion over the Himalayas) the additional criterion was applied that directly above the SOP the ozone mixing ratios are again lower (at least by 20%), so that selected profiles have a shape typical of SOPs, as shown in Fig. 2. These two conditions can be mathematically expressed as

$$\mathrm{AOMR}_{10\text{–}12\mathrm{km}} \geqslant 1.5 \text{ x } \mathrm{AOMR}_{0\text{–}6\mathrm{km}}$$

and

$$\mathrm{AOMR}_{12\text{–}14\mathrm{km}} \leqslant 0.8 \text{ x } \mathrm{AOMR}_{10\text{–}12\mathrm{km}}$$

Further, the factors 1.5 and 0.8 representing an enhancement by 50% and reduction by 20% were suitably varied, which confirmed the generality of the result (not shown). We calculated the frequencies of occurrence in percentage for each month during 2000–2014, and converted these to an average climatological seasonal cycle ~~, with the year-to-year variation shown as standard deviation (1-sigma)~~ (Fig. 11). Standard deviations in a month represents the variability in the SOP frequency among different years during 2000-2014 period.

The highest frequency of SOPs over the central Himalayas is found during the pre-monsoon season (MAM), followed by winter (DJF). The frequency of SOP occurrences over Nainital increases steadily from January (2.7%) to May (10.8%), and abruptly declines in June (1.2%). The model does not predict any SOPs during July–October. It should be noted that here we included only those events as SOPs, which show enhancements by at least 50%, therefore some events with smaller enhancements could be present during July–October. It is suggested that the more frequent stratospheric intrusions during spring, combined with the stronger horizontal advection, lead to more frequent SOP events. Seasonal composites of the spatial locations of folds (Fig. S6) shows higher frequency of

occurrence during SOPs. The effects of stronger cross-tropopause exchange and influx of the stratospheric air masses during spring and winter over the Himalayas and surrounding regions, such as southern parts of the Tibetan Plateau, have also been shown by Ŝkerlak et al. (2014, 2015). The frequency of SOP events over this region is minimum during the summer monsoon season, as the weak horizontal winds (Ojha et al., 2014; Naja et al., 2016) do not transport the ozone from STTs over large distances. The frequency of stratospheric intrusions and tropopause folds over the Himalayas and surrounding regions are lower during the summer monsoon (Cristofanelli et al., 2010; Putero et al., 2016). Multiple tropopauses that can occur in winter and spring over the Tibetan Plateau are shown to be absent during the summer monsoon season (Chen et al., 2011). Additionally, stronger vertical mixing due to monsoonal convection inhibits high ozone layers to form and sustain. These findings are in agreement with the ground-based ozone measurements in the southern Himalaya, where about 78% of the stratospheric influences were attributed to the PV structures ~~and subtropical jet streams~~induced by fluctuations of the zonal flow and tropopause fold development along the the subtropical jet-stream, while monsoon depressions only account for 3% of the events (Bracci et al., 2012). Further, the seasonality of SOP frequency derived from EMAC simulations is consistent with the conclusions based on the limited number of observational profiles in Ojha et al. (2014). Next we determine the enhancements in tropospheric ozone columns due to presence of SOPs over the central Himalayas.

3.4 Effect of SOPs on Tropospheric Column Ozone

Fig. 12 shows the climatological mean seasonal cycle of the Tropospheric Column Ozone (TCO) in Dobson Units (DU) over Nainital from EMAC simulations over the period 2000–2014. TCO values are calculated by integrating ozone mixing ratios up to the LRT, determined using the WMO definition. To investigate the effect of SOPs on TCO, we compare three TCO values: First using EMAC simulated O_3 values from all time steps, second by selecting only the time steps when there is an SOP event as per the criteria discussed in Sec. 3.3, and third by taking all time steps when SOPs do not occur.

TCO values for All-times and No-SOPs are found to be very similar, mainly due to the large number of data counts (more than 1000 data counts in individual month), as compared to those in SOPs (0-120 data counts in individual month). The maxima of TCO during May and June (54.7±5.9 and 55.0±4.4 DU respectively) are attributed to the intense solar radiation and high pollution loading over northern India. While photochemical production of ozone is less efficient during the winter (TCO: 33.7±3.6 to 37.6±5.8 DU) and the summer monsoon (e.g. 44.9±4.9 DU in August). Overall, the EMAC simulated TCO seasonality from all data is found to be consistent with satellite data (Ojha et al., 2012) over this region.

The occurrences of SOPs are seen to clearly enhance the TCO values during the winter, pre-monsoon and early summer. To estimate the enhancement in the tropospheric ozone that would

likely persist in the troposphere (not reversible), here an additional criterion of PV values upto 2 PVU has been applied.

The maximum enhancement in climatological average TCO value due to SOPs is found during January, when TCO values during SOPs (43.5±~~4.6~~ 3.0 DU) are higher by as much as ~~9 DU (26~~7.5 DU (21%) compared to the non-SOP time steps (~~34.5~~36.0±~~4.6~~ 3.6 DU). The enhancements in tropospheric ozone loading over the central Himalayas due to SOPs are estimated to be ~~4–9 DU (7–26~~3.3–7.5 DU (6–21%) during January to June. Additional calculations, relaxing the PV criteria to include SOP timesteps having PV values higher than 2PVU as well, shows slightly higher values of the estimated enhancement (4–9 DU: 7–26%) on the TCO.

4 Conclusions

In this study, we used the EMAC model to investigate the layers of high ozone mixing ratios (SOPs) in the middle-upper troposphere, observed over the central Himalayas in northern India. EMAC successfully reproduces the occurrence, altitudinal placement and the relative ozone enhancements during SOP events observed in ozonesonde profiles. The vertical profiles calculated by ~~EMAC~~ long-term EMAC simulations show layers of high PV (1.8~~–4.7~~ ±0.5 – 3.0±1.3 PVU) coinciding with the altitude of SOPs suggesting the influences from stratospheric intrusions. The analysis of O_3s further shows that generally all excess ozone at SOP altitudes over the Himalayas is transported from the stratosphere. ~~Photochemically produced (tropospheric)ozone is found to be significant only towards the onset of~~ Average O_3s at the SOP altitudes is estimated to be maximum during the spring (162.5±40 nmol mol^{-1}), followed by winter (149.4±35 nmol mol^{-1}). Tropospheric photochemical sources are found to contribute significantly to the SOPs and above during the summer monsoon (30 nmol mol^{-1}).

Analysis of backward air trajectories in conjunction with EMAC simulated O_3 distributions and tropopause dynamics revealed that stratospheric air masses are sandwiched between tropospheric layers at 10–11 km altitude due to tropopause folds which are rapidly transported along the subtropical jet to cause SOP structures over the Himalayas. In contrast to SOP timesteps, a fraction of air mass trajectories during non SOP timesteps are from the south west, which have significantly lower contributions of stratospheric ozone. Regions as far as northern Africa and the Atlantic Ocean, the Middle-East and northern South Asia are found to be regions of stratospheric intrusions that act as sources of high-ozone mixing ratios. The distribution of O_3s showed that STT effects ~~have been confined at latitudes higher than about 25°N and are minimal over the~~ are more pronounced over the northern Indian subcontinent than those over southern India.

We used long-term model simulations (2000–2014) to calculate the frequency of SOP occurrence showing maxima during spring (about 11% of the time in May), while no SOPs were predicted during the July–October months. This is consistent with results based on ozone soundings over the

region. The high frequency of SOPs during spring is attributed to the occurrence of stratospheric intrusions combined with rapid horizontal transport. The minima in the frequency of SOPs during the summer monsoon are partially due to much weaker horizontal transport ~~supplemented with~~ due to the northward displacement of subtropical jet stream and stronger monsoonal convective mixing. Model simulations were further used to investigate the effect of SOPs on the TCO. The EMAC simulated TCO seasonality is in agreement with satellite data. SOP occurrence is found to significantly enhance the TCO over the region by ~~4–9 DU (7–26~~3.3–7.5 DU (6–21%). Such an enhancement in tropospheric ozone at the SOP altitude could translate to an increase in surface temperature by 0.06 to 0.13 degree, based on the vertical profile of ozone forcing (Lacis et al., 1990). Additionally, as expected due to their origin from dynamical processes, the occurrences of SOPs discern very large interannual variability (see e. g. Supplementary material-Fig. S9), which highlights a need of in situ measurements and numerical simulations on climatic timescales to quantify the role of SOPs in measured ozone trends over Asian regions especially in the middle-upper troposphere (Banerjee et al., 2016; Tanimoto et al., 2016), and their impacts on tropospheric chemistry and climate.

Acknowledgements. The model simulations have been performed at the German Climate Computing Centre (DKRZ) through support from the Bundesministerium für Bildung und Forschung (BMBF). DKRZ and its scientific steering committee are gratefully acknowledged for providing the HPC and data archiving resources for this consortial project ESCiMo (Earth System Chemistry integrated Modelling). The authors gratefully acknowledge the NOAA Air Resources Laboratory (ARL) for the provision of the HYSPLIT transport and dispersion model and READY website (http://www.ready.noaa.gov) used in this publication. Constructive comments and suggestions from the two anonymous reviewers are gratefully acknowledged.

References

Akritidis, D., Pozzer, A., Zanis, P., Tyrlis, E., Škerlak, B., Sprenger, M., and Lelieveld, J.: On the role of tropopause folds in summertime tropospheric ozone over the eastern Mediterranean and the Middle East, Atmospheric Chemistry and Physics Discussions, 2016, 1–24, doi:10.5194/acp-2016-547, http://www.atmos-chem-phys-discuss.net/acp-2016-547/, 2016.

Banerjee, A., Maycock, A. C., Archibald, A. T., Abraham, N. L., Telford, P., Braesicke, P., and Pyle, J. A.: Drivers of changes in stratospheric and tropospheric ozone between year 2000 and 2100, Atmospheric Chemistry and Physics, 16, 2727–2746, doi:10.5194/acp-16-2727-2016, http://www.atmos-chem-phys.net/16/2727/2016/, 2016.

Bracci, A., Cristofanelli, P., Sprenger, M., Bonafè, U., Calzolari, F., Duchi, R., Laj, P., Marinoni, A., Roccato, F., Vuillermoz, E., and Bonasoni, P.: Transport of Stratospheric Air Masses to the Nepal Climate Observatory–Pyramid (Himalaya; 5079 m MSL): A Synoptic-Scale Investigation, Journal of Applied Meteorology and Climatology, 51, 1489–1507, doi:10.1175/JAMC-D-11-0154.1, 2012.

Chen, X. L., Ma, Y. M., Kelder, H., Su, Z., and Yang, K.: On the behaviour of the tropopause folding events over the Tibetan Plateau, Atmospheric Chemistry and Physics, 11, 5113–5122, doi:10.5194/acp-11-5113-2011, http://www.atmos-chem-phys.net/11/5113/2011/, 2011.

Cristofanelli, P., Bracci, A., Sprenger, M., Marinoni, A., Bonafè, U., Calzolari, F., Duchi, R., Laj, P., Pichon, J. M., Roccato, F., Venzac, H., Vuillermoz, E., and Bonasoni, P.: Tropospheric ozone variations at the Nepal Climate Observatory-Pyramid (Himalayas, 5079 m a.s.l.) and influence of deep stratospheric intrusion events, Atmospheric Chemistry and Physics, 10, 6537–6549, doi:10.5194/acp-10-6537-2010, http://www.atmos-chem-phys.net/10/6537/2010/, 2010.

Das, S. S., Ratnam, M. V., Uma, K. N., Subrahmanyam, K. V., Girach, I. A., Patra, A. K., Aneesh, S., Suneeth, K. V., Kumar, K. K., Kesarkar, A. P., Sijikumar, S., and Ramkumar, G.: Influence of tropical cyclones on tropospheric ozone: possible implications, Atmospheric Chemistry and Physics, 16, 4837–4847, doi:10.5194/acp-16-4837-2016, http://www.atmos-chem-phys.net/16/4837/2016/, 2016.

Dee, D. P., Uppala, S. M., Simmons, A. J., Berrisford, P., Poli, P., Kobayashi, S., Andrae, U., Balmaseda, M. A., Balsamo, G., Bauer, P., Bechtold, P., Beljaars, A. C. M., van de Berg, L., Bidlot, J., Bormann, N., Delsol, C., Dragani, R., Fuentes, M., Geer, A. J., Haimberger, L., Healy, S. B., Hersbach, H., Hólm, E. V., Isaksen, L., Kållberg, P., Köhler, M., Matricardi, M., McNally, A. P., Monge-Sanz, B. M., Morcrette, J.-J., Park, B.-K., Peubey, C., de Rosnay, P., Tavolato, C., Thépaut, J.-N., and Vitart, F.: The ERA-Interim reanalysis: configuration and performance of the data assimilation system, Quarterly Journal of the Royal Meteorological Society, 137, 553–597, doi:10.1002/qj.828, http://dx.doi.org/10.1002/qj.828, 2011.

Dobson, G.: The laminated structure of the ozone in the atmosphere, Quarterly Journal of the Royal Meteorological Society, 99, 599–607, 1973.

Draxler, R. and Hess, G.: Description of the HYSPLIT 4 modeling system, NOAA Tech. Memo. ERL ARL-224, NOAA Air Resources Laboratory, Silver Spring, MD, p. 24 pp., 1997.

Draxler, R. and Hess, G.: An overview of the HYSPLIT 4 modeling system of trajectories, dispersion, and deposition, Aust. Meteor. Mag., 47, 295–308, 1998.

Draxler, R., Stunder, B., Rolph, G., Stein, A., and Taylor, A.: HYSPLIT4 USER's GUIDE, http://www.arl.noaa.gov/documents/reports/hysplit_user_guide.pdf, 2014.

Ellrod, G. and Knapp, D.: An Objective Clear-Air Turbulence Forecasting Technique: Verification and Operational Use, Weather and Forecasting, 7, 150–165, doi:10.1175/1520-0434(1992)007<0150:AOCATF>2.0.CO;2, http://dx.doi.org/10.1175/1520-0434(1992)007<0150:AOCATF>2.0.CO;2, 1992.

Fadnavis, S., Chakraborty, T., and Beig, G.: Seasonal stratospheric intrusion of ozone in the upper troposphere over India, Annales Geophysicae, 28, 2149–2159, doi:10.5194/angeo-28-2149-2010, http://www.ann-geophys.net/28/2149/2010/, 2010.

Fishman, J., Wozniak, A. E., and Creilson, J. K.: Global distribution of tropospheric ozone from satellite measurements using the empirically corrected tropospheric ozone residual technique: Identification of the regional aspects of air pollution, Atmospheric Chemistry and Physics, 3, 893–907, doi:10.5194/acp-3-893-2003, http://www.atmos-chem-phys.net/3/893/2003/, 2003.

Ganguly, N. D. and Tzanis, C.: Study of Stratosphere-troposphere exchange events of ozone in India and Greece using ozonesonde ascents, Meteorological Applications, 18, 467–474, doi:10.1002/met.241, http://dx.doi.org/10.1002/met.241, 2011.

Holton, J. R. and Lelieveld, J.: Stratosphere-Troposphere Exchange and its role in the budget of tropospheric ozone, pp. 173–190, Springer Berlin Heidelberg, Berlin, Heidelberg, doi:10.1007/978-3-642-61051-6_8, http://dx.doi.org/10.1007/978-3-642-61051-6_8, 1996.

Hwang, S.-H., Kim, J., Won, Y.-I., Cho, H. K., Kim, J. S., Lee, D.-H., Cho, G.-R., and Oh, S. N.: Statistical characteristics of secondary ozone density peak observed in Korea, Advances in Space Research, 36, 952–957, doi:http://dx.doi.org/10.1016/j.asr.2005.05.080, http://www.sciencedirect.com/science/article/pii/S027311770500699X, 2005.

Hwang, S.-H., Kim, J., and Cho, G.-R.: Observation of secondary ozone peaks near the tropopause over the Korean peninsula associated with stratosphere-troposphere exchange, Journal of Geophysical Research: Atmospheres, 112, n/a–n/a, doi:10.1029/2006JD007978, http://dx.doi.org/10.1029/2006JD007978, d16305, 2007.

Jöckel, P., Kerkweg, A., Pozzer, A., Sander, R., Tost, H., Riede, H., Baumgaertner, A., Gromov, S., and Kern, B.: Development cycle 2 of the Modular Earth Submodel System (MESSy2), Geoscientific Model Development, 3, 717–752, doi:10.5194/gmd-3-717-2010, http://www.geosci-model-dev.net/3/717/2010/, 2010.

Jöckel, P., Tost, H., Pozzer, A., Kunze, M., Kirner, O., Brenninkmeijer, C. A. M., Brinkop, S., Cai, D. S., Dyroff, C., Eckstein, J., Frank, F., Garny, H., Gottschaldt, K.-D., Graf, P., Grewe, V., Kerkweg, A., Kern, B., Matthes, S., Mertens, M., Meul, S., Neumaier, M., Nützel, M., Oberländer-Hayn, S., Ruhnke, R., Runde, T., Sander, R., Scharffe, D., and Zahn, A.: Earth System Chemistry integrated Modelling (ESCiMo) with the Modular Earth Submodel System (MESSy) versionÂ 2.51, Geoscientific Model Development, 9, 1153–1200, doi:10.5194/gmd-9-1153-2016, http://www.geosci-model-dev.net/9/1153/2016/, 2016.

Kumar, A., Ram, K., and Ojha, N.: Variations in carbonaceous species at a high-altitude site in western India: Role of synoptic scale transport, Atmospheric Environment, pp. –, doi:http://dx.doi.org/10.1016/j.atmosenv.2015.07.039, http://www.sciencedirect.com/science/article/pii/S1352231015302387, 2015.

Lacis, A. A., Wuebbles, D. J., and Logan, J. A.: Radiative forcing of climate by changes in the vertical distribution of ozone, Journal of Geophysical Research: Atmospheres, 95, 9971–9981, doi:10.1029/JD095iD07p09971, http://dx.doi.org/10.1029/JD095iD07p09971, 1990.

519 Lal, S., Venkataramani, S., Srivastava, S., Gupta, S., Mallik, C., Naja, M., Sarangi, T., Acharya, Y. B., and Liu,
520 X.: Transport effects on the vertical distribution of tropospheric ozone over the tropical marine regions sur-
521 rounding India, Journal of Geophysical Research: Atmospheres, 118, 1513–1524, doi:10.1002/jgrd.50180,
522 http://dx.doi.org/10.1002/jgrd.50180, 2013.
523 Lelieveld, J. and Dentener, F. J.: What controls tropospheric ozone?, Journal of Geophysical Research: Atmo-
524 spheres, 105, 3531–3551, doi:10.1029/1999JD901011, http://dx.doi.org/10.1029/1999JD901011, 2000.
525 Lemoine, R.: Secondary maxima in ozone profiles, Atmospheric Chemistry and Physics, 4, 1085–1096,
526 doi:10.5194/acp-4-1085-2004, http://www.atmos-chem-phys.net/4/1085/2004/, 2004.
527 Logan, J. A.: Tropospheric ozone: :Seasonal behavior, trends and antropogenic influence, J. Geophys. Res., 90,
528 10 463–10 482, 1985.
529 Logan, J. A.: Trends in the vertical distribution of ozone: an analysis of ozonesonde data, J. Geophys. Res., 99,
530 25 553–25 585, 1994.
531 Ma, J., Lin, W. L., Zheng, X. D., Xu, X. B., Li, Z., and Yang, L. L.: Influence of air mass downward
532 transport on the variability of surface ozone at Xianggelila Regional Atmosphere Background Station,
533 southwest China, Atmospheric Chemistry and Physics, 14, 5311–5325, doi:10.5194/acp-14-5311-2014,
534 http://www.atmos-chem-phys.net/14/5311/2014/, 2014.
535 Mandal, T. K., Cho, J. Y. N., Rao, P. B., Jain, A. R., Peshin, S. K., Srivastava, S. K., Bohra, A. K., and Mitra,
536 A. P.: Stratosphere-troposphere ozone exchange observed with the Indian MST radar and a simultaneous
537 balloon-borne ozonesonde, Radio Science, 33, 861–893, doi:10.1029/97RS03553, http://dx.doi.org/10.1029/
538 97RS03553, 1998.
539 Monks, P. S., Archibald, A. T., Colette, A., Cooper, O., Coyle, M., Derwent, R., Fowler, D., Granier, C., Law,
540 K. S., Mills, G. E., Stevenson, D. S., Tarasova, O., Thouret, V., von Schneidemesser, E., Sommariva, R., Wild,
541 O., and Williams, M. L.: Tropospheric ozone and its precursors from the urban to the global scale from air
542 quality to short-lived climate forcer, Atmospheric Chemistry and Physics, 15, 8889–8973, doi:10.5194/acp-
543 15-8889-2015, http://www.atmos-chem-phys.net/15/8889/2015/, 2015.
544 Myhre, G., Shindell, D., Breon, F.-M., Collins, W., Fuglestvedt, J., Huang, J., Koch, D., Lamarque, J.-F.,
545 Lee, D., Mendoza, B., Nakajima, T., Robock, A., Stephens, G., Takemura, T., and Zhang, H.: Anthro-
546 pogenic and Natural Radiative Forcing. In: Climate Change 2013: The Physical Science Basis. Contri-
547 bution of Working Group I to the Fifth Assessment Report of the Intergovernmental Panel on Climate
548 Change [Stocker, T.F., D. Qin, G.-K. Plattner, M. Tignor, S.K. Allen, J. Boschung, A. Nauels, Y. Xia, V.
549 Bex and P.M. Midgley (eds.)], Cambridge University Press, https://www.ipcc.ch/pdf/assessment-report/ar5/
550 wg1/WG1AR5_Chapter08_FINAL.pdf, 2013.
551 Naja, M., Bhardwaj, P., Singh, N., Kumar, P., Kumar, R., Ojha, N., Sagar, R., Satheesh, S. K., Krishna Moorthy,
552 K., and Kotamarthi, V. R.: High-frequency vertical profiling of meteorological parameters using AMF1 facil-
553 ity during RAWEX-GVAX at ARIES, Nainital, Curr. Sci., 110, 2317–2325, doi:10.18520/cs/v110/i12/2317-
554 2325, 2016.
555 Neu, J. L., Flury, T., Manney, G. L., Santee, M. L., Livesey, N. J., and Worden, J.: Tropospheric ozone
556 variations governed by changes in stratospheric circulation, NATURE GEOSCIENCE, 7, 340–344,
557 doi:10.1038/NGEO2138, 2014.

Ojha, N., Naja, M., Singh, K. P., Sarangi, T., Kumar, R., Lal, S., Lawrence, M. G., Butler, T. M., and Chandola, H. C.: Variabilities in ozone at a semi-urban site in the Indo-Gangetic Plain region: Association with the meteorology and regional processes, Journal of Geophysical Research: Atmospheres, 117, doi:10.1029/2012JD017716, http://dx.doi.org/10.1029/2012JD017716, 2012.

Ojha, N., Naja, M., Sarangi, T., Kumar, R., Bhardwaj, P., Lal, S., Venkataramani, S., Sagar, R., Kumar, A., and Chandola, H.: On the processes influencing the vertical distribution of ozone over the central Himalayas: Analysis of yearlong ozonesonde observations, Atmospheric Environment, 88, 201–211, doi:http://dx.doi.org/10.1016/j.atmosenv.2014.01.031, http://www.sciencedirect.com/science/article/pii/S1352231014000491, 2014.

Ojha, N., Pozzer, A., Rauthe-Schöch, A., Baker, A. K., Yoon, J., Brenninkmeijer, C. A. M., and Lelieveld, J.: Ozone and carbon monoxide over India during the summer monsoon: regional emissions and transport, Atmospheric Chemistry and Physics, 16, 3013–3032, doi:10.5194/acp-16-3013-2016, http://www.atmos-chem-phys.net/16/3013/2016/, 2016.

Park, S. S., Kim, J., Cho, H. K., Lee, H., Lee, Y., and Miyagawa, K.: Sudden increase in the total ozone density due to secondary ozone peaks and its effect on total ozone trends over Korea, Atmospheric Environment, 47, 226 – 235, doi:http://dx.doi.org/10.1016/j.atmosenv.2011.11.011, http://www.sciencedirect.com/science/article/pii/S1352231011011745, 2012.

Pozzer, A., Jöckel, P., Tost, H., Sander, R., Ganzeveld, L., Kerkweg, A., and Lelieveld, J.: Simulating organic species with the global atmospheric chemistry general circulation model ECHAM5/MESSy1: a comparison of model results with observations, Atmospheric Chemistry and Physics, 7, 2527–2550, doi:10.5194/acp-7-2527-2007, http://www.atmos-chem-phys.net/7/2527/2007/, 2007.

Pozzer, A., Pollmann, J., Taraborrelli, D., Jöckel, P., Helmig, D., Tans, P., Hueber, J., and Lelieveld, J.: Observed and simulated global distribution and budget of atmospheric C_2–C_5 alkanes, Atmospheric Chemistry and Physics, 10, 4403–4422, doi:10.5194/acp-10-4403-2010, http://www.atmos-chem-phys.net/10/4403/2010/, 2010.

Pozzer, A., de Meij, A., Pringle, K. J., Tost, H., Doering, U. M., van Aardenne, J., and Lelieveld, J.: Distributions and regional budgets of aerosols and their precursors simulated with the EMAC chemistry-climate model, Atmospheric Chemistry and Physics, 12, 961–987, doi:10.5194/acp-12-961-2012, http://www.atmos-chem-phys.net/12/961/2012/, 2012.

Putero, D., Cristofanelli, P., Sprenger, M., Škerlak, B., Tositti, L., and Bonasoni, P.: STEFLUX, a tool for investigating stratospheric intrusions: application to two WMO/GAW global stations, Atmospheric Chemistry and Physics Discussions, 2016, 1–23, doi:10.5194/acp-2016-514, http://www.atmos-chem-phys-discuss.net/acp-2016-514/, 2016.

Ramanathan, V., Ramana, M. V., Roberts, G., Kim, D., Corrigan, C., Chung, C., and Winker, D.: Warming trends in Asia amplified by brown cloud solar absorption, Nature, 448, doi:10.1038/nature06019, http://dx.doi.org/10.1038/nature06019, 2007.

Ramanathan, V., Agrawal, M., Akimoto, H., Aufhammer, M., Devotta, S., Emberson, L., Hasnain, S. I., Iyngararasan, M., Jayaraman, A., Lawrance, M., Nakajima, T., Oki, T., Rodhe, H., Ruchirawat, M., Tan, S. K., Vincent, J., Y., W. J., Yang, D., Zhang, Y. H., Autrup, H., Barregard, L., Bonasoni, P., Brauer, M., Brunekreef, B., Carmichael, G., Chung, C. E., Dahe, J., Feng, Y., Fuzzi, S., Gordon, T., Gosain, A. K., Htun, N., Kim, J.,

Mourato, S., Naeher, L., Navasumrit, P., Ostro, B., Panwar, T., Rahman, M. R., Ramana, M. V., Rupakheti, M., Settachan, D., Singh, A. K., Helen, G. S., Tan, P. V., Viet, P. H., Yinlong, J., Yoon, S. C., Chang, W.-C., Wang, X., Zelikoff, J., and Zhu, A.: Atmospheric Brown Clouds: Regional Assessment Report with Focus on Asia, United Nations Environment Programme, Nairobi, Kenya., 2008.

Reid, S. J. and Vaughan, G.: Lamination in ozone profiles in the lower stratosphere, Quarterly Journal of the Royal Meteorological Society, 117, 825–844, 1991.

Roeckner, E., Brokopf, R., Esch, M., Giorgetta, M., Hagemann, S., Kornblueh, L., Manzini, E., Schlese, U., and Schulzweida, U.: Sensitivity of Simulated Climate to Horizontal and Vertical Resolution in the ECHAM5 Atmosphere Model, Journal of Climate, 19, 3771–3791, doi:10.1175/JCLI3824.1, http://dx.doi.org/10.1175/JCLI3824.1, 2006.

Roelofs, G.-J. and Lelieveld, J.: Model study of the influence of cross-tropopause O3 transports on tropospheric O3 levels, Tellus B, 49, 38–55, doi:10.1034/j.1600-0889.49.issue1.3.x, http://dx.doi.org/10.1034/j.1600-0889.49.issue1.3.x, 1997.

Sarangi, T., Naja, M., Ojha, N., Kumar, R., Lal, S., Venkataramani, S., Kumar, A., Sagar, R., and Chandola, H. C.: First simultaneous measurements of ozone, CO, and NOy at a high-altitude regional representative site in the central Himalayas, Journal of Geophysical Research: Atmospheres, 119, 1592–1611, doi:10.1002/2013JD020631, http://dx.doi.org/10.1002/2013JD020631, 2014.

Shindell, D., Kuylenstierna, J. C. I., Vignati, E., van Dingenen, R., Amann, M., Klimont, Z., Anenberg, S. C., Muller, N., Janssens-Maenhout, G., Raes, F., Schwartz, J., Faluvegi, G., Pozzoli, L., Kupiainen, K., Höglund-Isaksson, L., Emberson, L., Streets, D., Ramanathan, V., Hicks, K., Oanh, N. T. K., Milly, G., Williams, M., Demkine, V., and Fowler, D.: Simultaneously Mitigating Near-Term Climate Change and Improving Human Health and Food Security, Science, 335, 183–189, doi:10.1126/science.1210026, http://science.sciencemag.org/content/335/6065/183, 2012.

Singh, N., Solanki, R., Ojha, N., Janssen, R. H. H., Pozzer, A., and Dhaka, S. K.: Boundary layer evolution over the central Himalayas from Radio Wind Profiler and Model Simulations, Atmospheric Chemistry and Physics Discussions, 2016, 1–33, doi:10.5194/acp-2016-101, http://www.atmos-chem-phys-discuss.net/acp-2016-101/, 2016.

Sinha, P., Sahu, L., Manchanda, R., Sheel, V., Deushi, M., Kajino, M., Schultz, M., Nagendra, N., Kumar, P., Trivedi, D., Koli, S., Peshin, S., Swamy, Y., Tzanis, C., and Sreenivasan, S.: Transport of tropospheric and stratospheric ozone over India: Balloon-borne observations and modeling analysis, Atmospheric Environment, 131, 228 – 242, doi:http://dx.doi.org/10.1016/j.atmosenv.2016.02.001, http://www.sciencedirect.com/science/article/pii/S1352231016300905, 2016.

Ŝkerlak, B., Sprenger, M., and Wernli, H.: A global climatology of stratosphere-troposphere exchange using the ERA-Interim data set from 1979 to 2011, Atmospheric Chemistry and Physics, 14, 913–937, doi:10.5194/acp-14-913-2014, http://www.atmos-chem-phys.net/14/913/2014/, 2014.

Ŝkerlak, B., Sprenger, M., Pfahl, S., Tyrlis, E., and Wernli, H.: Tropopause folds in ERA-Interim: Global climatology and relation to extreme weather events, Journal of Geophysical Research: Atmospheres, 120, 4860–4877, doi:10.1002/2014JD022787, http://dx.doi.org/10.1002/2014JD022787, 2014JD022787, 2015.

Smit, H. G. J., Straeter, W., Johnson, B. J., Oltmans, S. J., Davies, J., Tarasick, D. W., Hoegger, B., Stubi, R., Schmidlin, F. J., Northam, T., Thompson, A. M., Witte, J. C., Boyd, I., and Posny, F.: Assessment of the

performance of ECC-ozonesondes under quasi-flight conditions in the environmental simulation chamber: Insights from the Juelich Ozone Sonde Intercomparison Experiment (JOSIE), Journal of Geophysical Research: Atmospheres, 112, n/a–n/a, doi:10.1029/2006JD007308, http://dx.doi.org/10.1029/2006JD007308, d19306, 2007.

Sprenger, M., Croci Maspoli, M., and Wernli, H.: Tropopause folds and cross-tropopause exchange: A global investigation based upon ECMWF analyses for the time period March 2000 to February 2001, Journal of Geophysical Research: Atmospheres, 108, n/a–n/a, doi:10.1029/2002JD002587, http://dx.doi.org/10.1029/2002JD002587, 8518, 2003.

Tanimoto, H., Zbinden, R., Thouret, V., and Nédélec, P.: Consistency of tropospheric ozone observations made by different platforms and techniques in the global databases, Tellus B, 67, http://www.tellusb.net/index.php/tellusb/article/view/27073, 2015.

Tanimoto, H., Ikeda, K., Okamoto, S., Thouret, V., Emmons, L., Tilmes, S., and Lamarque, J.-F.: Recent changes in the free tropospheric ozone over East Asian Pacific rim, International Global Atmospheric Chemistry (IGAC) Science Conference, 26-30 September 2016, Breckenridge, CO, USA, http://www.igac2016.org/IGAC2016_Abstracts/5.099_TANIMOTO.pdf, 2016.

Traub, M. and Lelieveld, J.: Cross-tropopause transport over the eastern Mediterranean, Journal of Geophysical Research: Atmospheres, 108, n/a–n/a, doi:10.1029/2003JD003754, http://dx.doi.org/10.1029/2003JD003754, 4712, 2003.

Trickl, T., Bärtsch-Ritter, N., Eisele, H., Furger, M., Mücke, R., Sprenger, M., and Stohl, A.: High-ozone layers in the middle and upper troposphere above Central Europe: potential import from the stratosphere along the subtropical jet stream, Atmospheric Chemistry and Physics, 11, 9343–9366, doi:10.5194/acp-11-9343-2011, http://www.atmos-chem-phys.net/11/9343/2011/, 2011.

Tyrlis, E., Škerlak, B., Sprenger, M., Wernli, H., Zittis, G., and Lelieveld, J.: On the linkage between the Asian summer monsoon and tropopause fold activity over the eastern Mediterranean and the Middle East, Journal of Geophysical Research: Atmospheres, 119, 3202–3221, doi:10.1002/2013JD021113, http://dx.doi.org/10.1002/2013JD021113, 2014.

Varotsos, C., Kalabokas, P., and Chronopoulos, G.: Association of the Laminated Vertical Ozone Structure with the Lower-Stratospheric Circulation, Journal of Applied Meteorology, 33, 473–476, 1994.

Venkat Ratnam, M., Ravindra Babu, S., Das, S. S., Basha, G., Krishnamurthy, B. V., and Venkateswararao, B.: Effect of tropical cyclones on the stratosphere-troposphere exchange observed using satellite observations over the north Indian Ocean, Atmospheric Chemistry and Physics, 16, 8581–8591, doi:10.5194/acp-16-8581-2016, http://www.atmos-chem-phys.net/16/8581/2016/, 2016.

Table 1. A comparison of average ozone mixing ratios between ozonesondes and EMAC model for the lower, middle and upper troposphere during the six SOP events over Nainital

Date	2–7 km		7–12 km		12–17 km	
	Sonde	EMAC	Sonde	EMAC	Sonde	EMAC
20110211	50.7±4.1	69.5±3.6	85.8±52.1	112.3±52.3	135.9±22.9	173.7±42.6
20110310	67.6±8.1	86.8±1.8	120.5±52.0	134.8±39.0	131.9±57.4	184.7±76.9
20110420	85.8±7.7	96.9±7.0	147.1±37.3	136.8±28.6	151.4±41.6	151.0±36.7
20110509	83.0±13.3	101.6±5.3	104.8±34.7	154.8±25.3	132.9±15.4	140.7±17.7
20110607	83.1±7.6	107.0±6.1	132.4±30.2	110.2±10.0	119.8±21.6	111.9±35.2
20111025	57.1±3.3	72.3±1.7	84.4±26.8	86.7±17.2	123.3±37.6	130.4±31.7

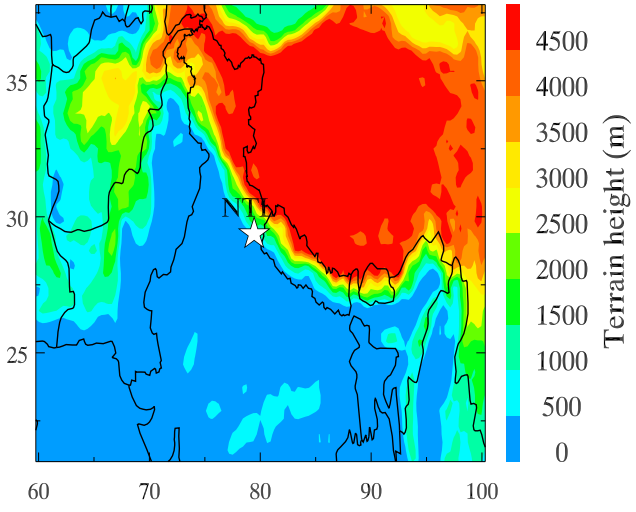

Figure 1. ~~(a) A typical Secondary Ozone Peak (SOP) in an ozonesonde profile measured at 10–11 km altitude on 10th March 2011 over Nainital (Ojha et al., 2014). (b)~~ Location of Nainital site in the central Himalayas shown in the topography map of the northern Indian region.

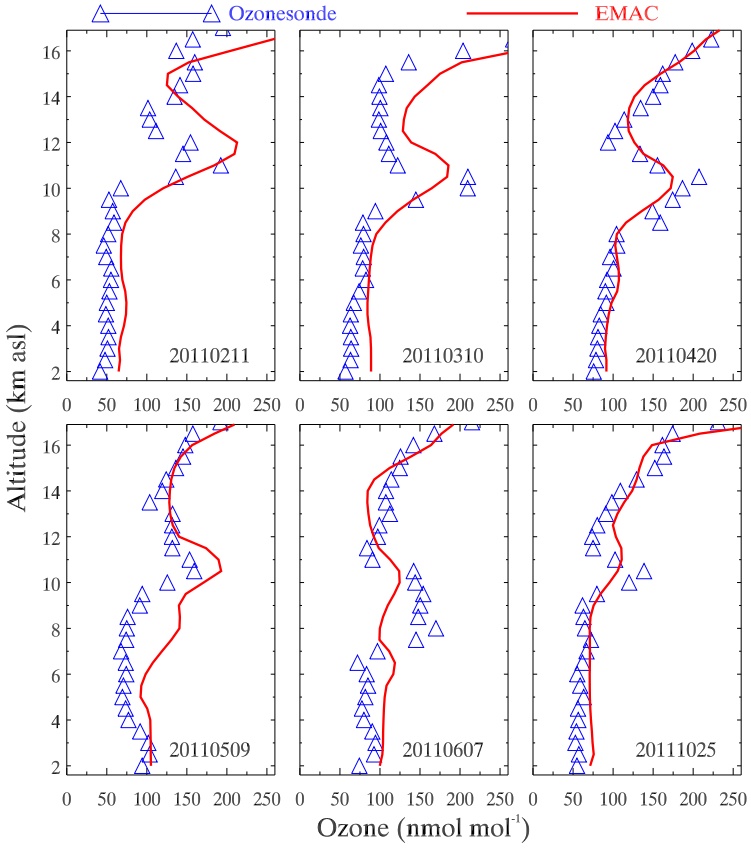

Figure 2. Comparison of EMAC simulated ozone profiles during the days of SOP events with ozonesonde observations over Nainital.

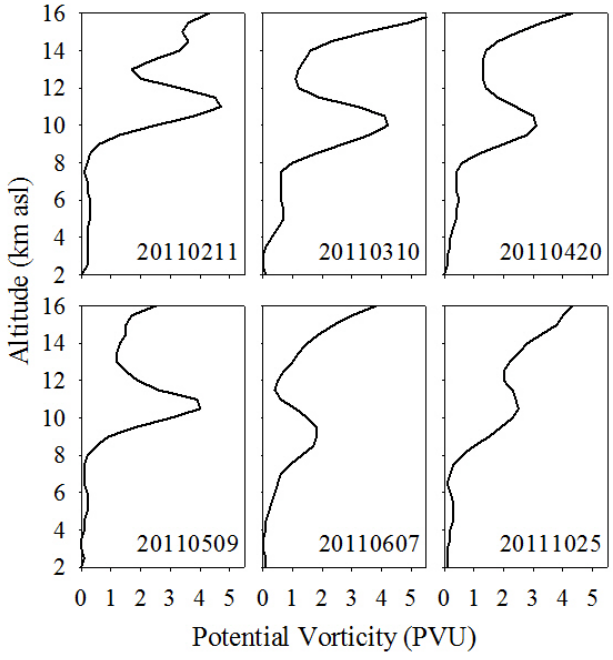

Figure 3. Vertical profiles of potential vorticity (PV) from EMAC simulations during the SOPs over Nainital.

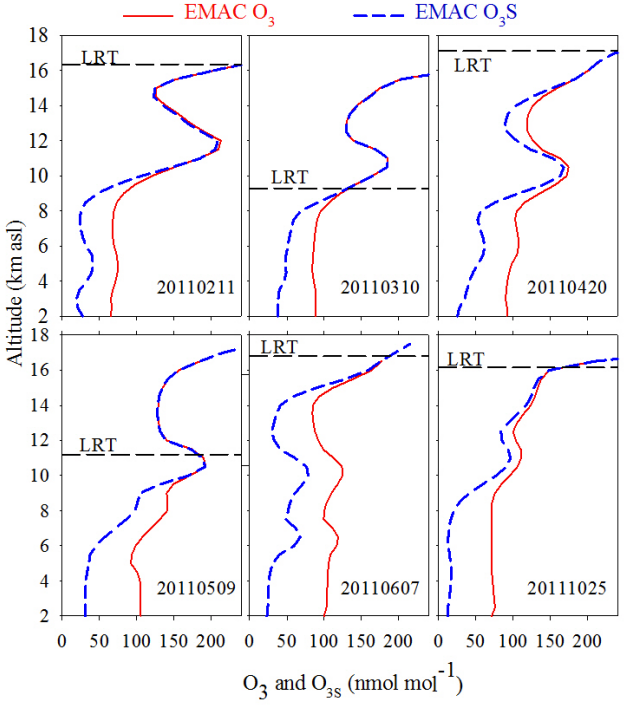

Figure 4. Vertical profiles of EMAC simulated ozone and stratospheric ozone tracer (O_3s) during the SOPs over Nainital. The height of the Lapse Rate Tropopause (LRT) from EMAC, calculated using the WMO definition, is also shown.

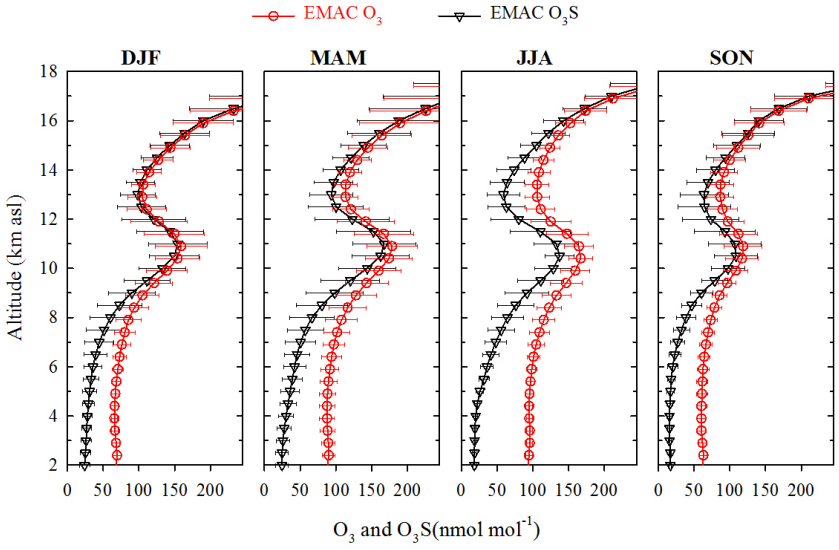

Figure 5. ~~Backward air trajectories over Nainital for all events, with starting altitude~~ Average vertical profiles of ~~10, 11~~ EMAC simulated ozone (O_3) and ~~12 km. The difference between symbols on trajectories represent a time period of 1 day. The locations of tropopause folds 5 days prior to~~ stratospheric ozone tracer (O_3s) during the ~~event obtained from EMAC simulations are also shown. The location of~~ SOPs over Nainital ~~site is shown by the star symbol. Small green circles represent shallow tropopause folds and bigger green circles~~ aggregated into four seasons: DJF (~~such as on 11th Feb~~Winter)~~represent medium tropopause folds~~ , MAM (~~see Sec. 3.2 for details~~Spring/ pre-monsoon), JJA (summer monsoon), and SON (autumn) for the period 2000–2014.

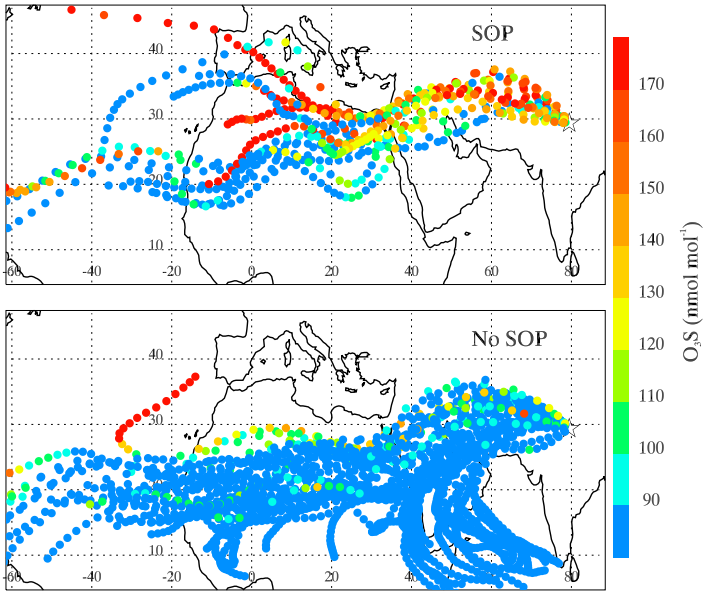

Figure 6. EMAC simulated evolution of O_3s along 5-day backward air trajectories over Nainital during SOPs and No SOPs with starting altitude of 11 km for the month May 2002. The difference between symbols on trajectories represent a time period of 3h. The location of the Nainital site is shown by the star symbol.

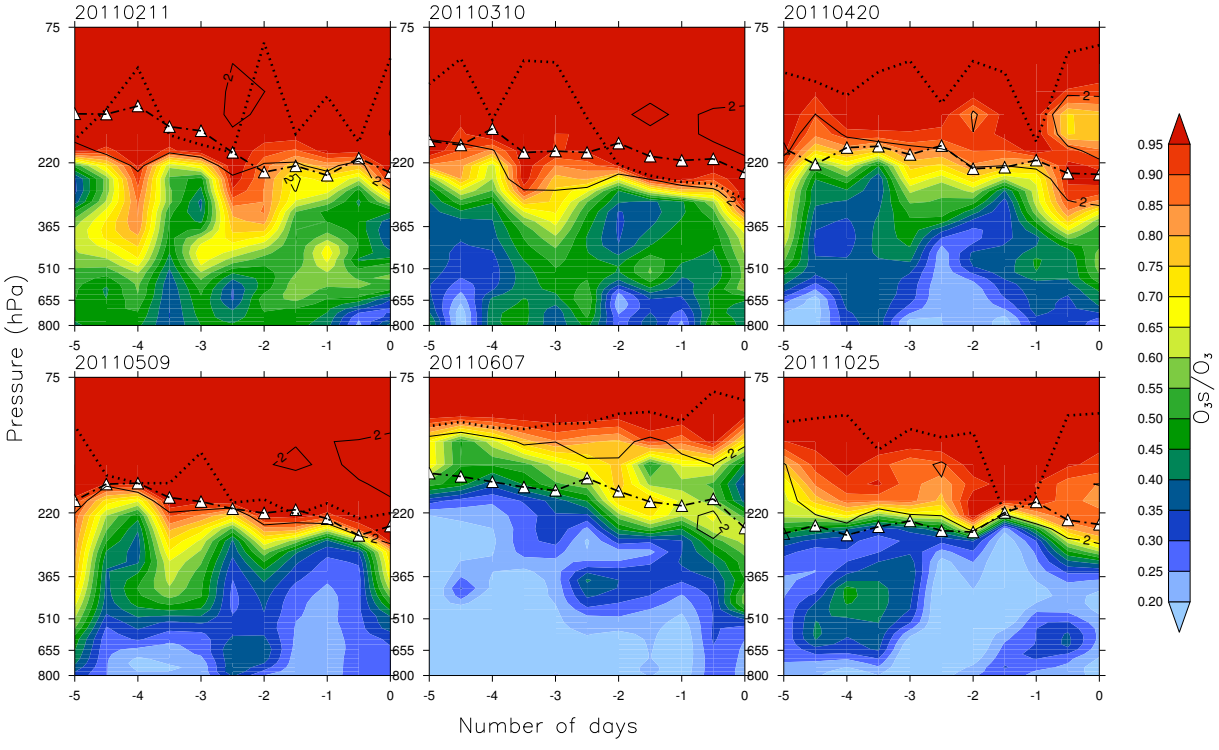

Figure 7. The vertical distribution of EMAC simulated O_3/O_3s ratio along the trajectories with starting altitude of 11km over Nainital. The X axis shows the number of days ~~back~~ backward in time and the Y axis shows the pressure in hPa. ~~The~~ White filled triangles show the pressure along the back-trajectory and the difference between two ~~black circles here represents~~ consecutive symbols on the line represent a time period of 12 h. The ~~white~~ dotted black line indicates the tropopause (LRT). The solid black line is the 2PVU contour.

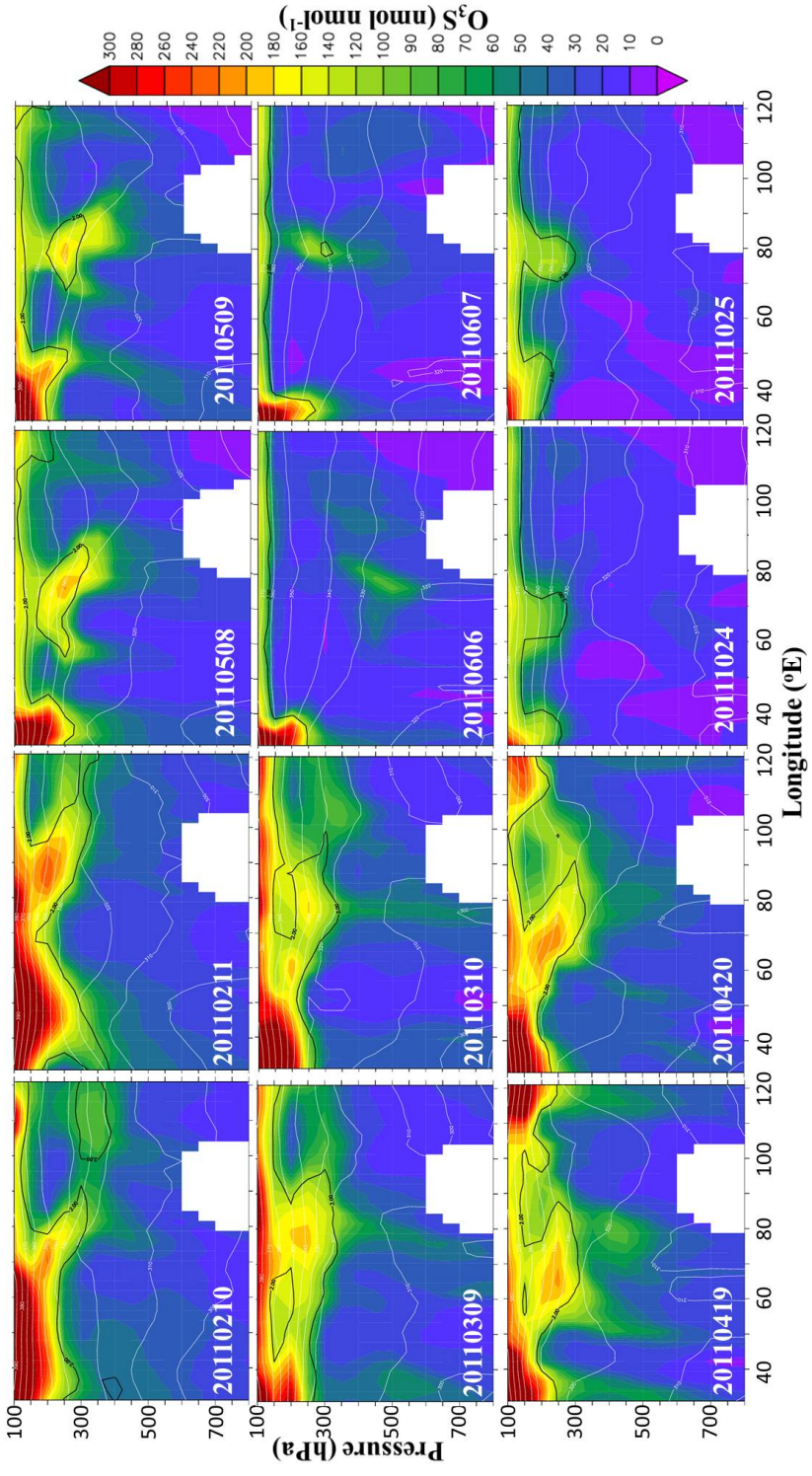

Figure 8. The longitude-pressure cross section of EMAC simulated O_3s at 29.5°N during all SOP days and a day before the event. White lines denote the potential temperature (K) and the black line denotes the dynamical tropopause at 2 PVU.

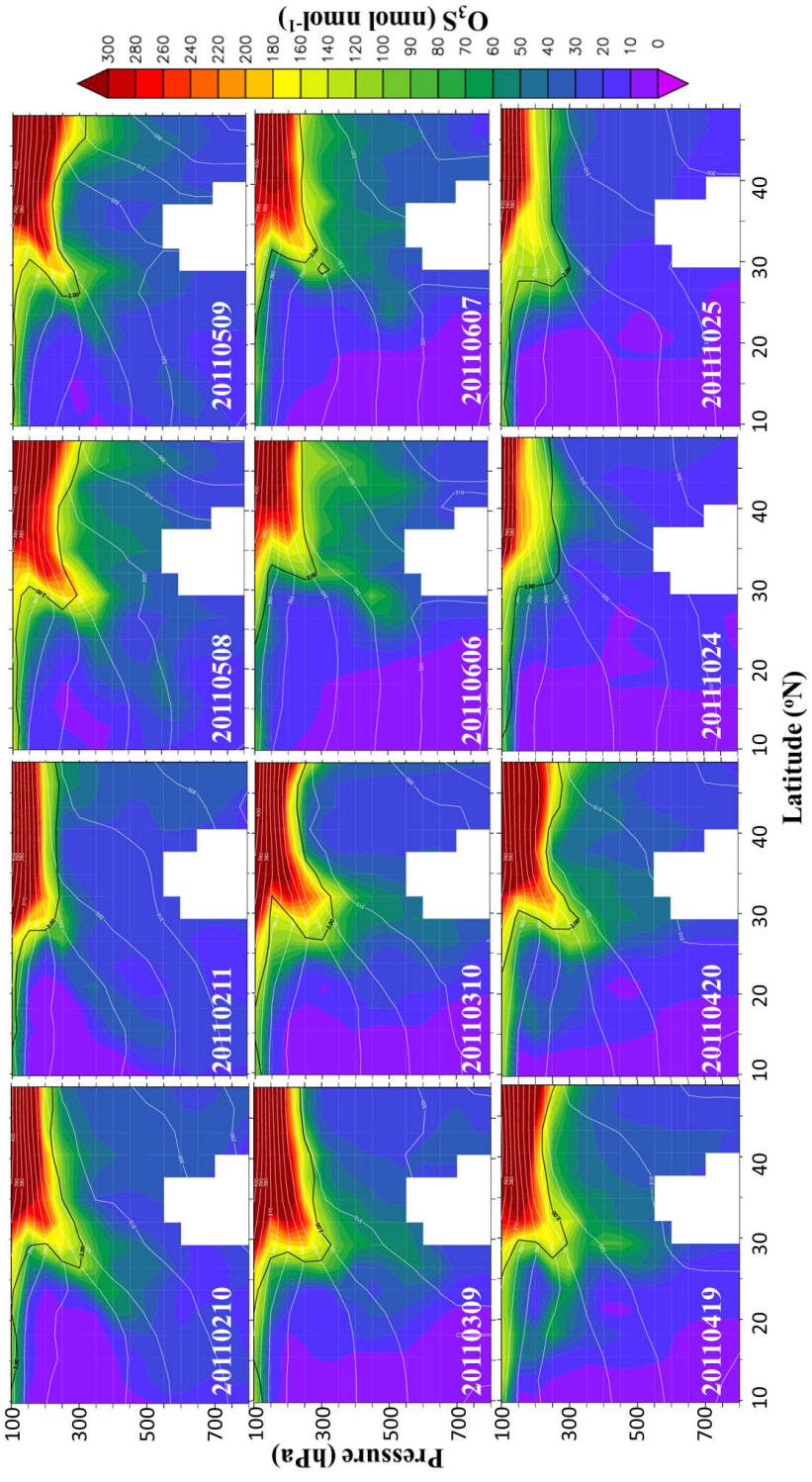

Figure 9. The latitude-pressure cross section of EMAC simulated O_{3S} at 79.5°E during all SOP days and a day before the event. White lines denote the potential temperature (K) and the black line denotes the dynamical tropopause at 2 PVU.

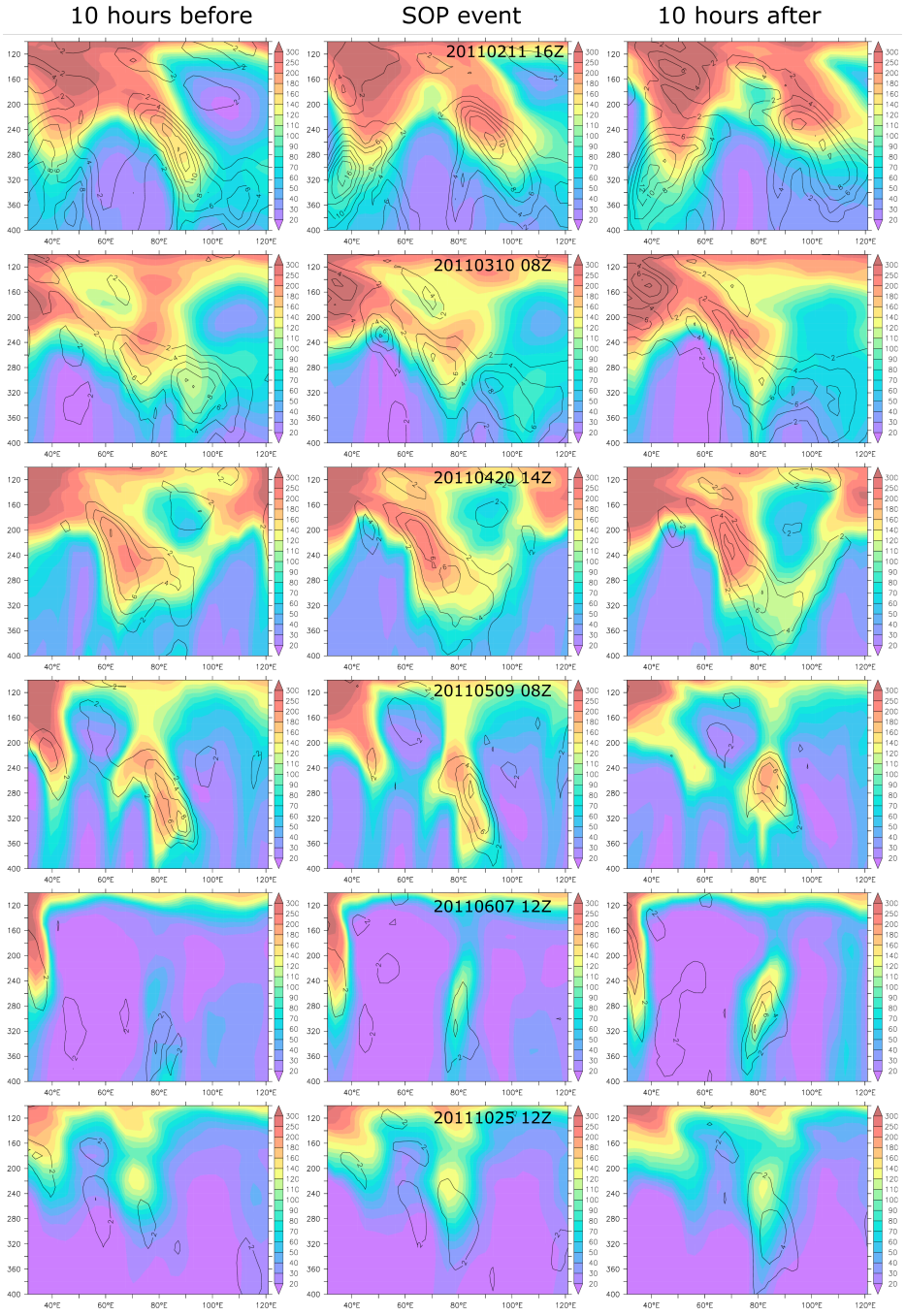

Figure 10. The longitude-pressure cross section of O_3s (color filled), and Turbulence Index (TI) (contour lines) (in $10^{-7}s^{-2}$) at 29.5°N.

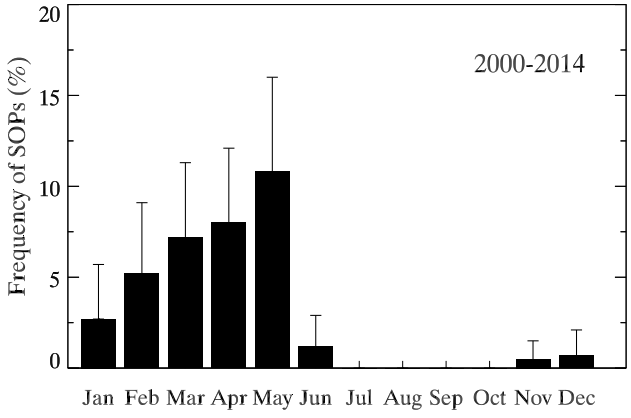

Figure 11. Annual cycle of ~~SOPs~~ SOP occurrence frequency (%) over Nainital, calculated from the EMAC simulations for the period 2000–2014. The error bars show the standard deviation of SOP frequency during each month among different years 2000-2014 period.

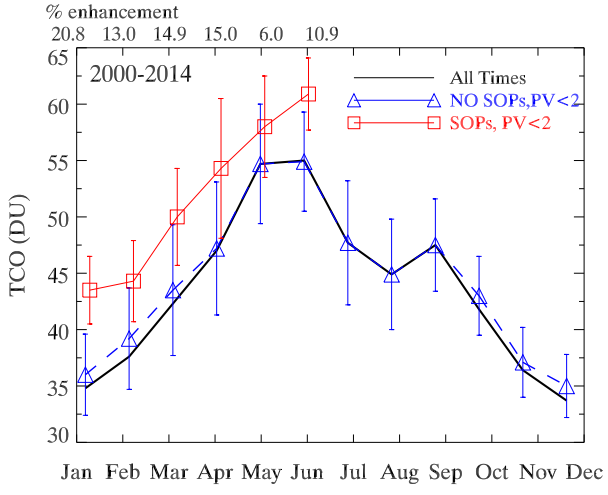

Figure 12. Annual cycle of EMAC simulated TCO over the central Himalayas calculated from 1) all EMAC time steps (All Times), 2) only the time steps having SOPs (SOPs), and 3) only when SOPs are not present (No SOPs) over the period 2000–2014. Enhancements in TCO values (in %) during SOPs as compared to No SOPs are also indicated. TCO values for SOPs and No SOPs are derived only when the average PV value at 10–12 km is up to 2PVU. Error bars represent the standard deviation derived from the temporal variations over the period of 2000-2014.